Relativistic Hydrodynamics in the context of the Hadron-Quark Phase Transition in Compact Stars

Matthias Hanauske, Goethe-University, Germany

1. Introduction
2. The Hadron-Quark Phase Transition in the Interior of Compact Stars
3. Astrophysical Observables for the Quark-Gluon Plasma
4. Relativistic Hydrodynamics and Numerical General Relativity

Pulsars ⟷ Compact Stars

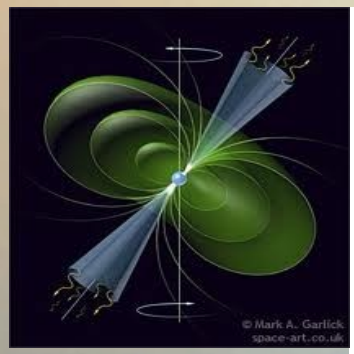

PSR B0329+54 (0.715 s)

PSR B0531+21 (33.5 ms)

PSR B1937+21 (1.56 ms)

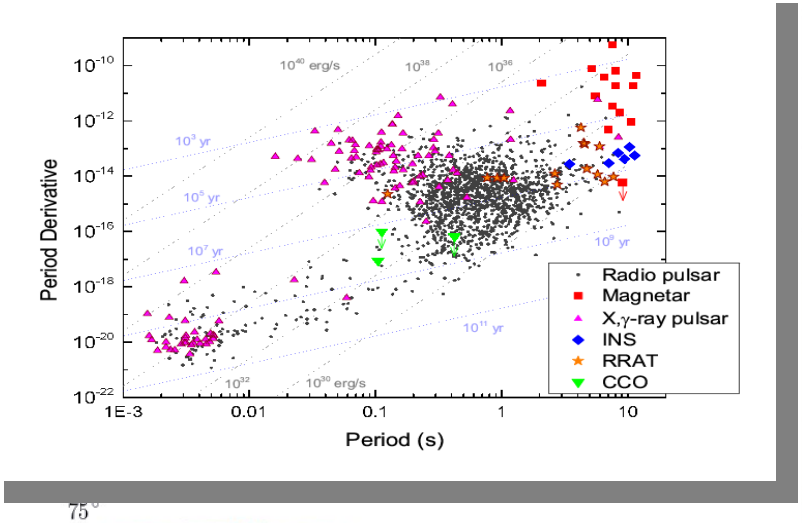

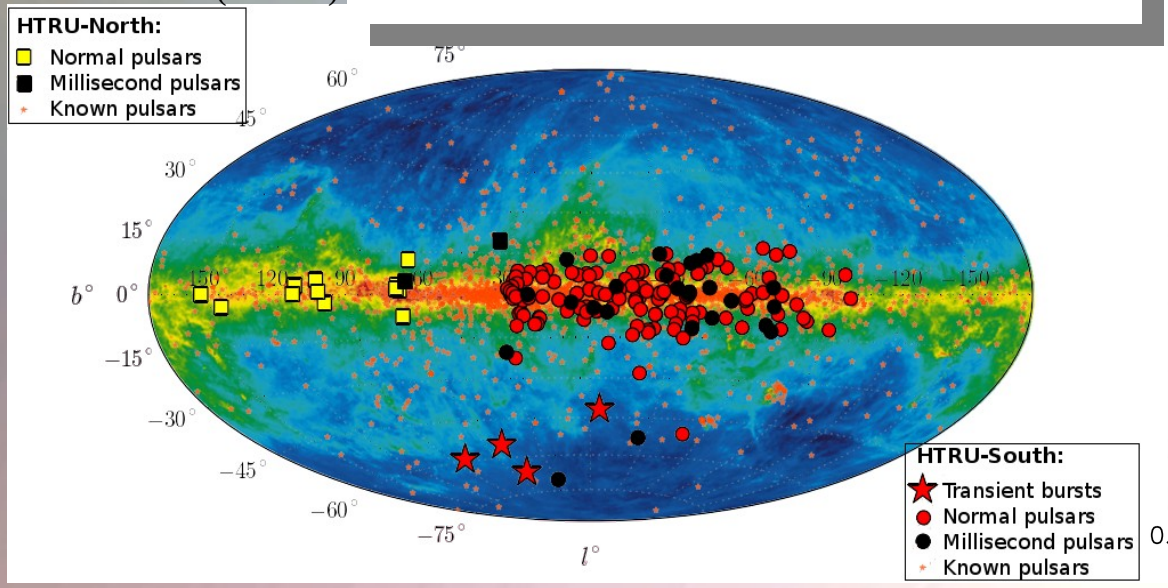

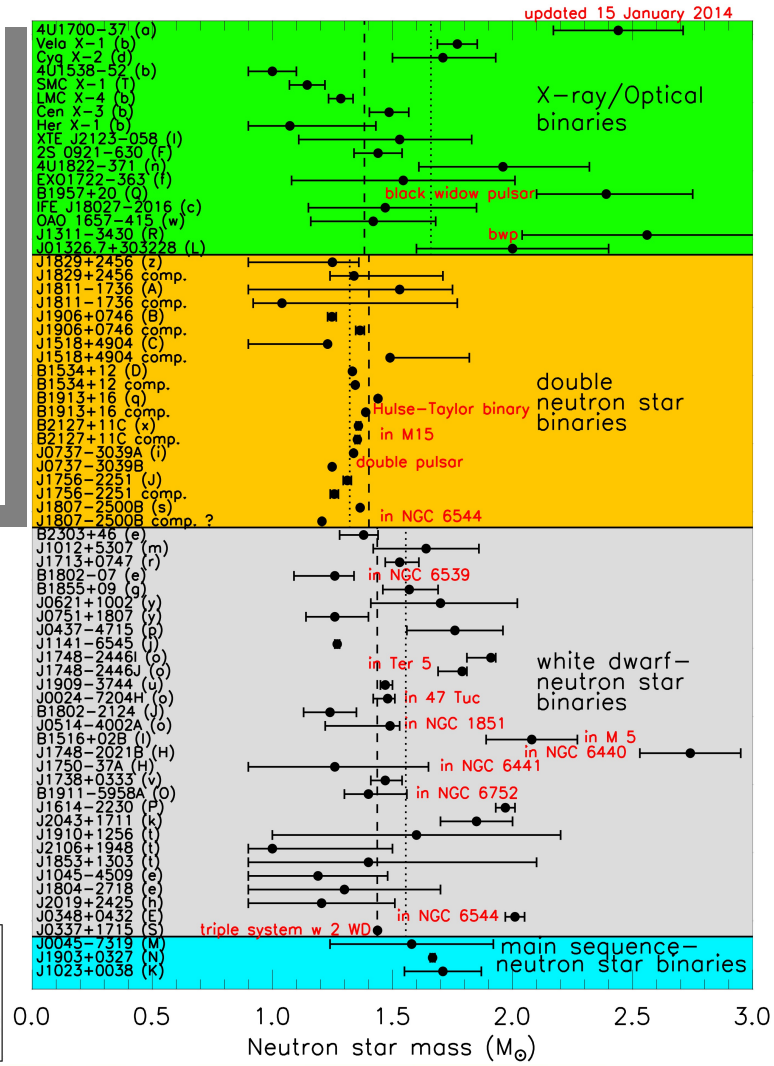

General Relativity and Quantum Cromodynamics

ART	Yang-Mills-Theories
$D_\beta v^\alpha = \partial_\beta\, v^\alpha + \Gamma^\alpha_{\sigma\beta}\, v^\sigma$	$D_{\beta a}{}^{b} = \partial_\beta\, 1_a{}^b + ig\, A_{\beta a}{}^b$
$R^\delta{}_{\mu\alpha\beta}\, v^\mu = [D_\alpha, D_\beta]\, v^\delta$	$F_{\alpha\beta a}{}^b = \frac{1}{ig}\left[D_{\alpha a}{}^c, D_{\beta c}{}^b\right]$
$R^\delta{}_{\mu\alpha\beta} = \Gamma^\delta_{\mu\alpha\vert\beta} - \Gamma^\delta_{\mu\beta\vert\alpha}$	$= A_{\beta a}{}^b{}_{\vert\alpha} - A_{\alpha a}{}^b{}_{\vert\beta}$
$+\Gamma^\delta_{\nu\beta}\Gamma^\nu_{\mu\alpha} + \Gamma^\delta_{\nu\alpha}\Gamma^\nu_{\mu\beta}$	$+\frac{1}{ig}\left[A_{\alpha a}{}^c, A_{\beta c}{}^b\right]$
$\mathcal{L}_G = R + \underbrace{(c_1\, R_{\mu\nu}R^{\mu\nu} + ...)}_{\equiv 0 \text{ for ART}}$	$\mathcal{L}_{YM} = \frac{1}{4} F_{\mu\nu a}{}^b\, F^{\mu\nu}{}_a{}^b$

QuantumCromoDynamic:

$(SU(3)_{(c)}$- Color Yang-Mills-Gauge Theory)

$$D_{\beta A}{}^B = \partial_\beta\, 1_A{}^B + ig\, G_{\beta A}{}^B$$

$_A{}^B$ =red, green, blue

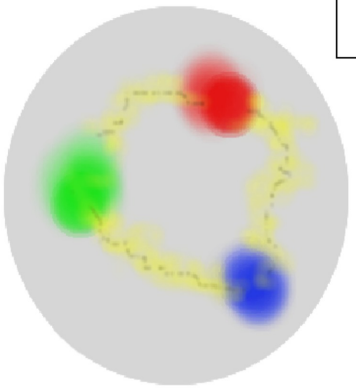

$$\psi^f_A = \begin{pmatrix} \psi^f_r \\ \psi^f_g \\ \psi^f_b \end{pmatrix}$$

Confinement

chiral symmetry, ...

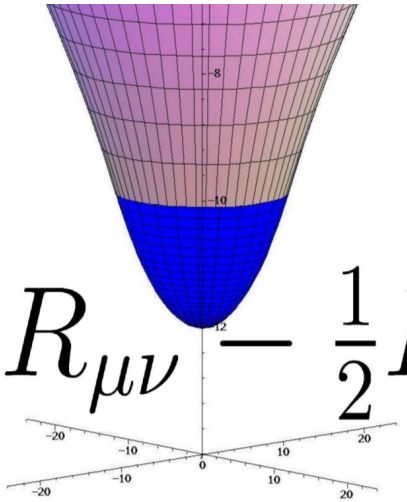

$$R_{\mu\nu} - \frac{1}{2} R\, g_{\mu\nu} = \frac{8\pi G}{c^4} T_{\mu\nu}$$

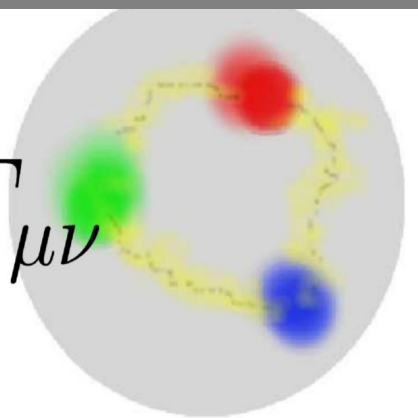

The QCD- Phase Diagram I

The QCD phase diagram at temperature T and net baryon density is displayed on the right side.

Some regions can be accessed by heavy ion collisions at different energies.

Matter of the early universe and in the interior of compact stars are also indicated within the diagram.

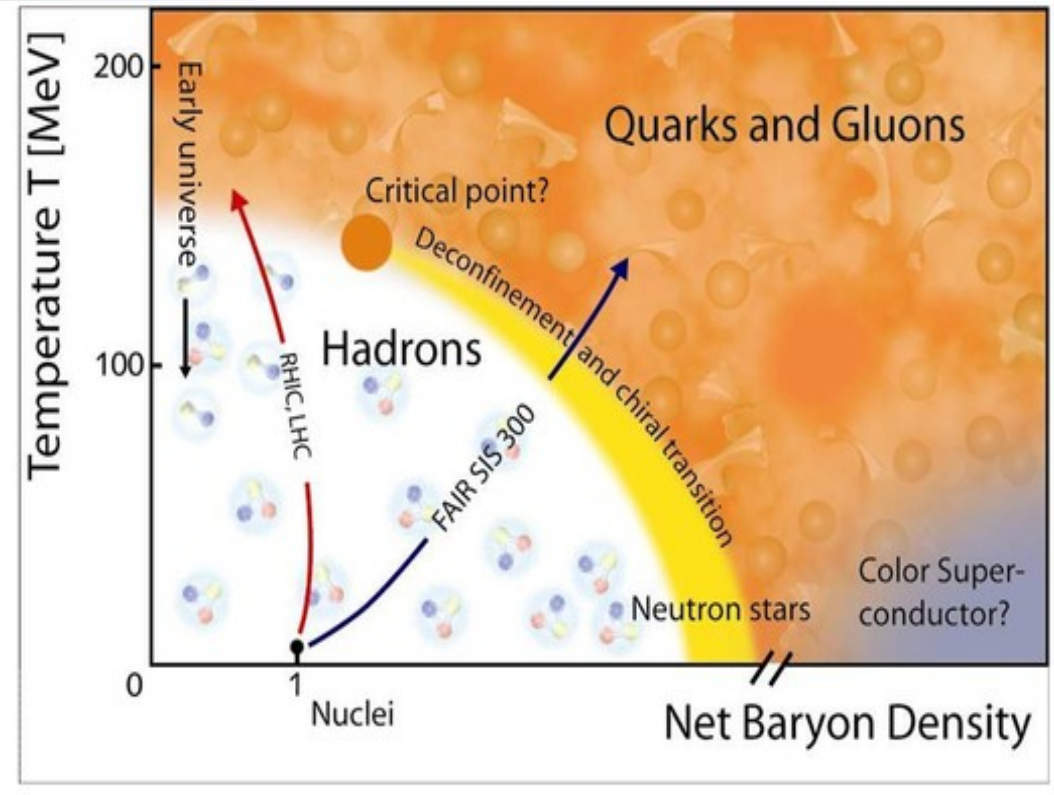

Image from
http://webarchiv.fz-juelich.de/nic/Publikationen/Broschuere/Elementarteilchenphysik/hadron.jpg

The QCD- Phase Diagram II

The QCD phase diagram at temperature T and net baryon density is displayed on the right side.

Some regions can be accessed by heavy ion collisions at different energies.

Matter of the early universe and in the interior of compact stars are also indicated within the diagram.

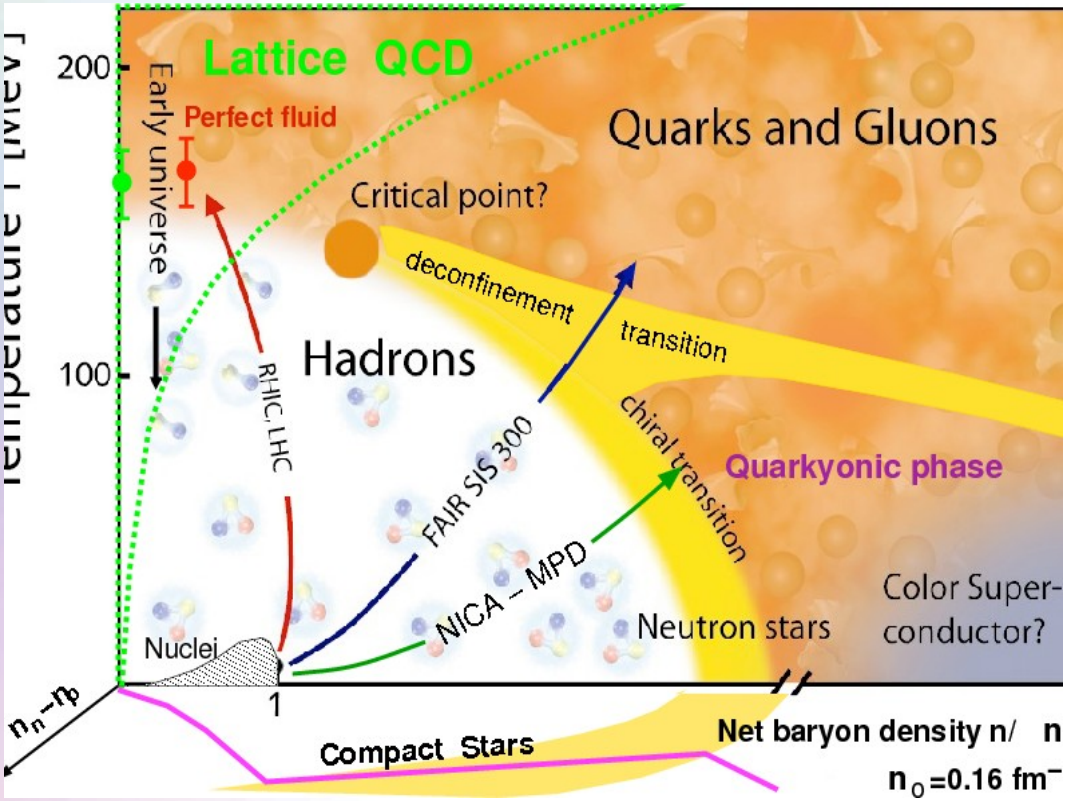

Image from
http://inspirehep.net/record/823172/files/phd_qgp3D_quarkyonic2.png

The QCD – Phase Transition

The appearance of the QCD - phase transition (the transition from confined hadronic to deconfined quark matter) will change the properties of neutron stars. Whether this change will be visible with telescopes and gravitational wave antennas depends strongly on the equation of state of hadronic and quark matter and on the construction of the phase transition.

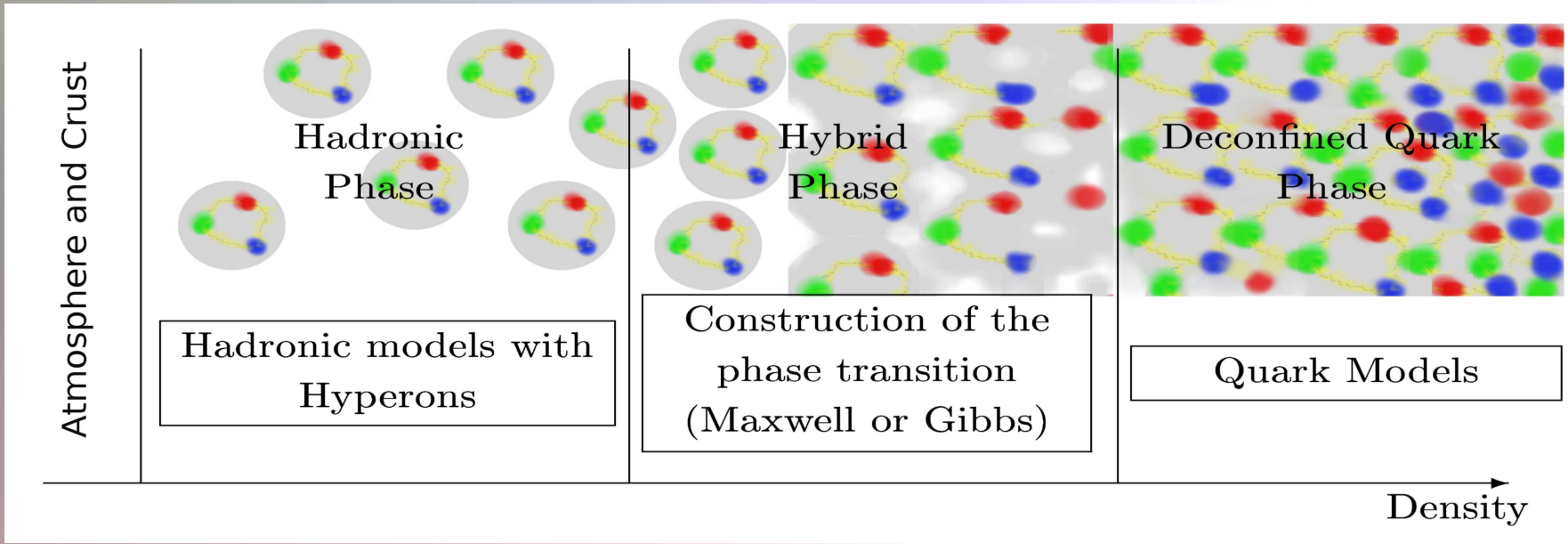

The Compact Star Zoo

Depending on the model used, the compact star zoo consists of different inhabitants: e.g. neutron stars with and without hyperons, quark stars and strange quark stars, hybrid stars with color superconducting quark matter, hybrid stars with Bose-Einstein condensates of antikaons.

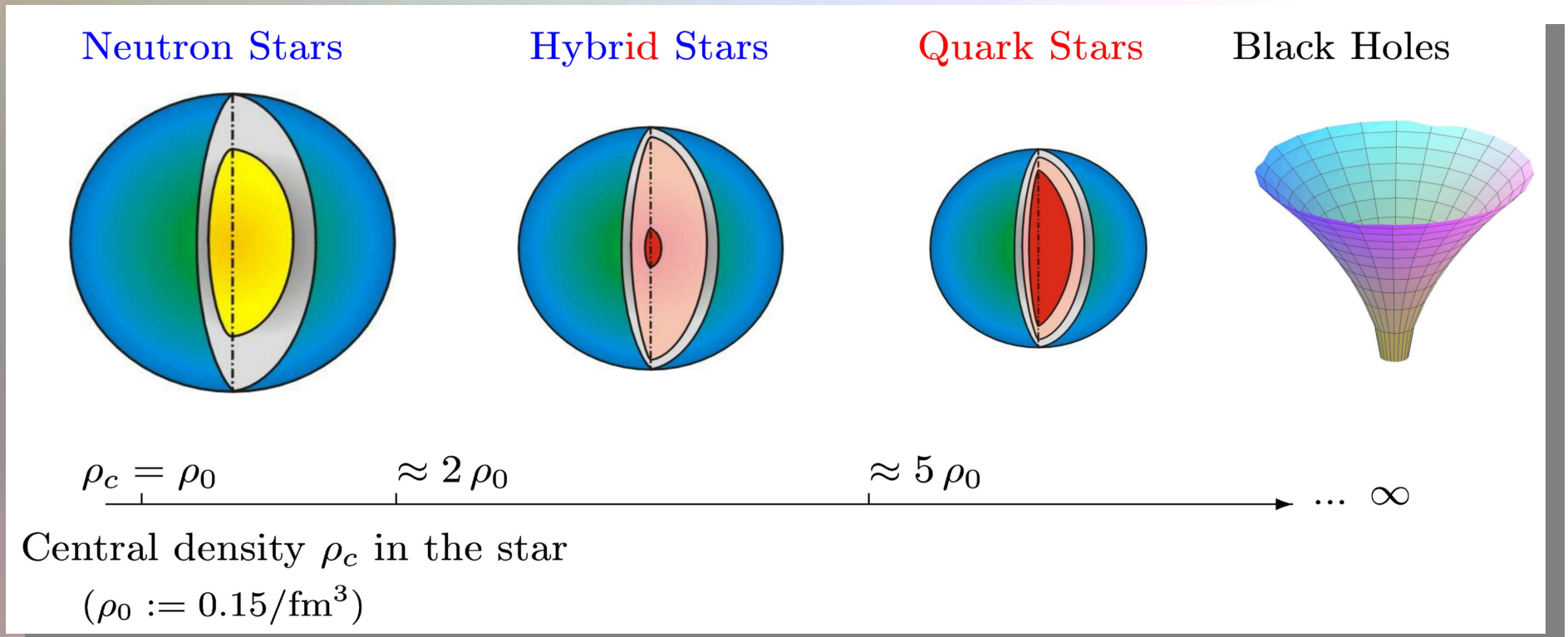

Neutron Stars (NS)

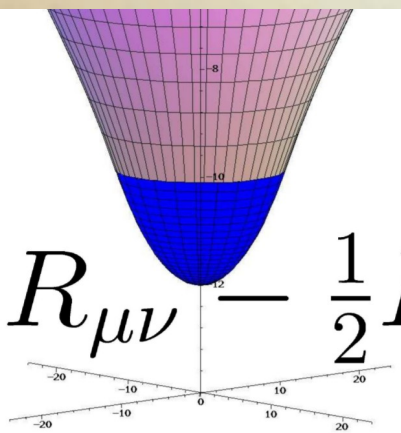

$$R_{\mu\nu} - \frac{1}{2} R\, g_{\mu\nu} = \frac{8\pi G}{c^4} T_{\mu\nu}$$

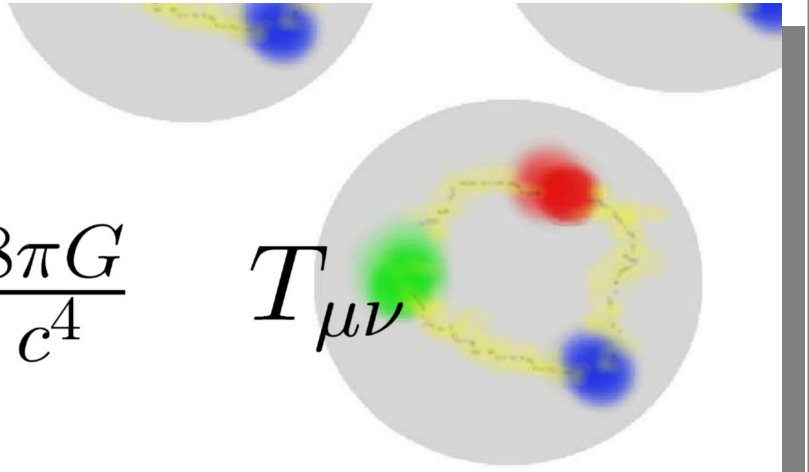

$$g_{\mu\nu} = \begin{pmatrix} e^{\nu(r)} & 0 & 0 & 0 \\ 0 & -\left(1 - \frac{2\,m(r)}{r}\right)^{-1} & 0 & 0 \\ 0 & 0 & -r^2 & 0 \\ 0 & 0 & 0 & -r^2 \sin^2\theta \end{pmatrix}$$

$$\begin{aligned} \mathcal{L} &= \sum_B \overline{\psi}_B \left(i\partial\!\!\!/ - m_B\right) \psi_B + \frac{1}{2}\partial^\mu\sigma\partial_\mu\sigma - \frac{1}{2}m_\sigma^2\sigma^2 - \frac{a}{3}\sigma^3 - \frac{b}{4}\sigma^4 - \frac{1}{4}\omega^{\mu\nu}\omega_{\mu\nu} \\ &\quad + \frac{1}{2}m_\omega^2\omega^\mu\omega_\mu - \frac{1}{4}\vec{\rho}^{\,\mu\nu}\vec{\rho}_{\mu\nu} + \frac{1}{2}m_\rho^2\vec{\rho}^{\,\mu}\vec{\rho}_\mu \\ &\quad + \sum_B \overline{\psi}_B \left(g_{\sigma B}\sigma + g_{\omega B}\omega^\mu\gamma_\mu + g_\rho\vec{\rho}^{\,\mu}\gamma_\mu\vec{\tau}_B\right)\psi_B \end{aligned}$$

Tolman-Oppenheimer-Volkoff Equation

$$\begin{aligned} \frac{dP}{dr} &= -\frac{(\epsilon + P)4\pi r^3 + m}{r(r - 2\,m)} \\ m(r) &= \int_0^r 4\pi\tilde{r}^2\epsilon(\tilde{r})\; d\tilde{r} \\ \frac{d\nu}{dr} &= \frac{8\pi P r^3 + 2\,m}{r(r - 2\,m)} \quad , \end{aligned}$$

Relativistic Mean-Field Hadronic Models

$$\mathcal{L}_{\rm lep} = \sum_{l=e,\mu} \overline{\psi}_l[i\gamma_\mu\partial^\mu - m_l]\psi_l$$

$$\begin{aligned} \mathcal{L}^{YY} &= \frac{1}{2}\left(\partial^\mu\sigma^*\partial_\mu\sigma^* - m_{\sigma^*}^2\sigma^{*2}\right) - \frac{1}{4}\phi^{\mu\nu}\phi_{\mu\nu} + \frac{1}{2}m_\phi^2\phi^\mu\phi_\mu \\ &\quad + \sum_Y \overline{\psi}_Y \left(g_{\sigma^* Y}\sigma^* + g_{\phi Y}\phi^\mu\gamma_\mu\right)\psi_Y \quad , \end{aligned}$$

Neutron Star Matter

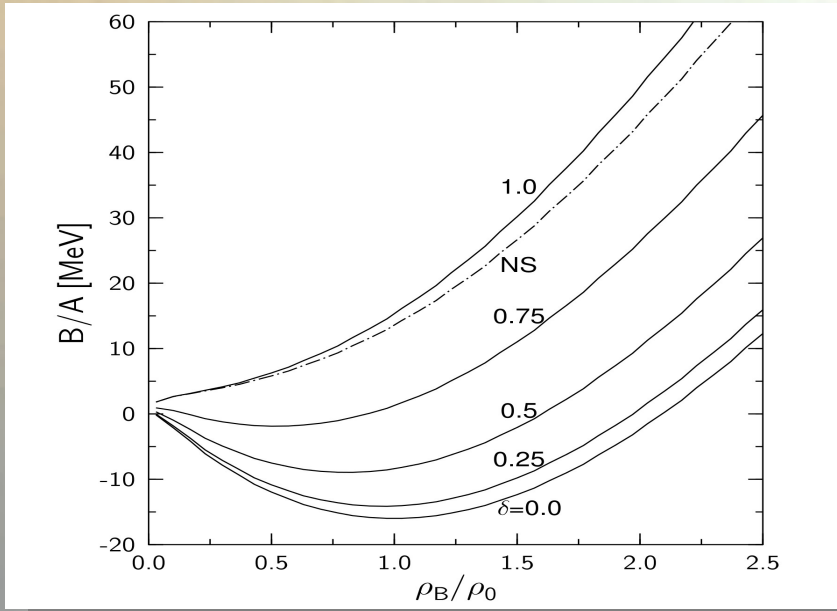

Binding energy per nucleon as a function of the baryonic density for different values of the neutron-proton asymmetry δ. 'NS' describes charge-neutral neutron star matter in β-equilibrium.

In contrast to normal nuclear matter, neutron star matter needs to fulfil three additional conditions:

1) Charge Neutrality
2) β-equilibrium $n \Leftrightarrow p + e + \tilde{\nu}_e$
3) Strangeness production

$$N + N \Rightarrow N + H + M \ ,$$

1) The equation of state (pressure P of the hadronic matter vs. the baryonic density). The solid curve (npe) describes charge-neutral matter in β-equilibrium consisting of neutrons, protons and electrons, whereas the dotted curve (npeμY) includes muons and hyperons.

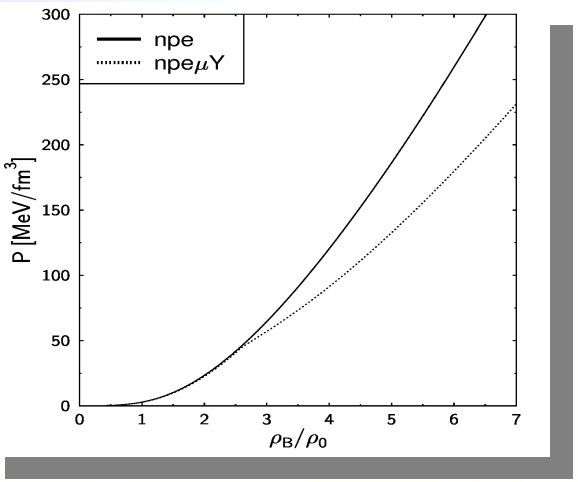

Particle Composition inside a NS

Relative particle composition in dependence of the baryonic density.

Λ-Hyperon	$n + n \leftrightarrow n + \Lambda + K^0$	$\mu_\Lambda = \mu_n$
Σ^--Hyperon	$n + n \leftrightarrow n + \Sigma^- + K^+$	$\mu_{\Sigma^-} = \mu_n + \mu_{e^-}$

Chemical potentials and single particle energies of hyperons in dependence of the baryonic density.

$$E_i(k) = E_i^*(k) + g_{i\omega}\omega_0 + g_{i\phi}\phi_0 + g_{i\rho}I_{3i}\rho_0 \,, \quad E_i^*(k) = \sqrt{k_i^2 + m_i^{*2}} \,,$$
$$\mu_i = b_i\mu_n - q_i\mu_e = \mu_i^* + g_{i\omega}\omega_0 + g_{i\phi}\phi_0 + g_{i\rho}I_{3i}\rho_0 \,, \qquad (3.9)$$

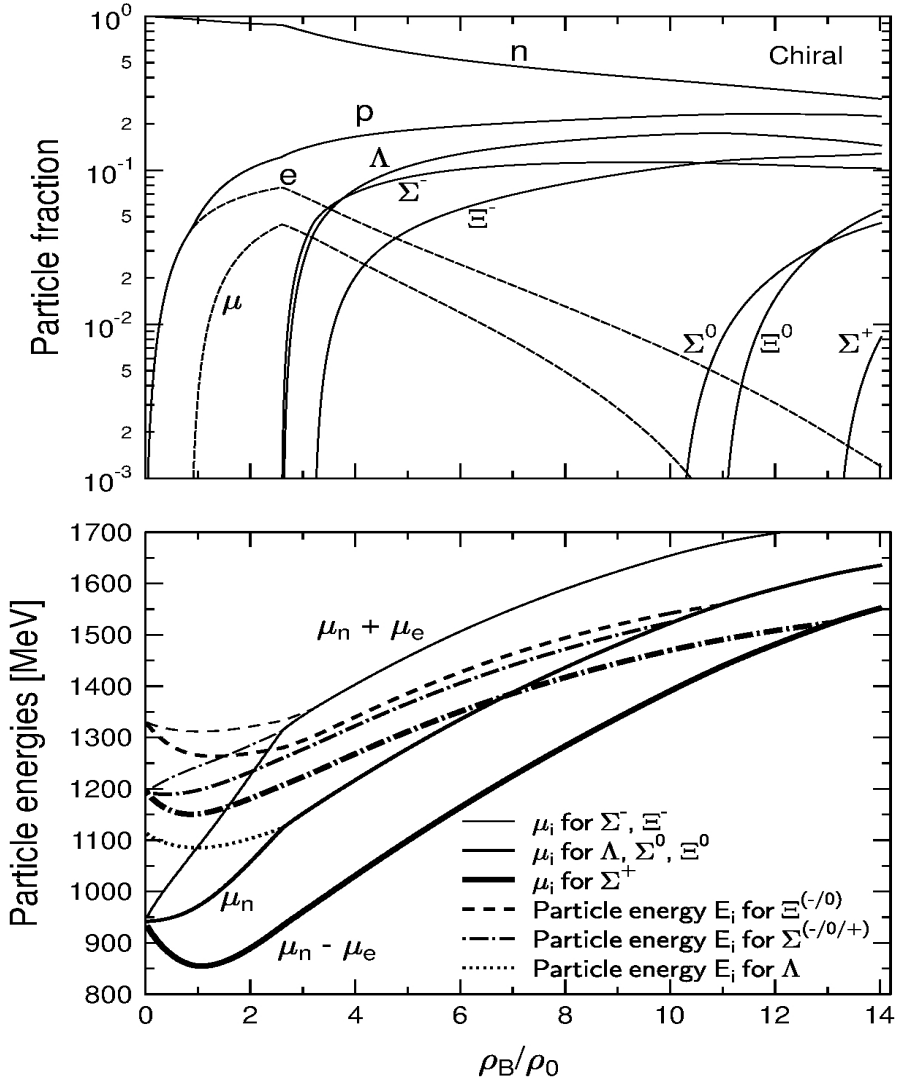

M. Hanauske, D. Zschiesche, S. Pal, S. Schramm, H. Stöcker, and W. Greiner, Astrophys. J. 537, 958 (2000)

Neutron Star Properties

The neutron star radius as a function of its mass. A low, middle and high density star is displayed within the figure. Additionally the onset of hyperonic particles is visualized.

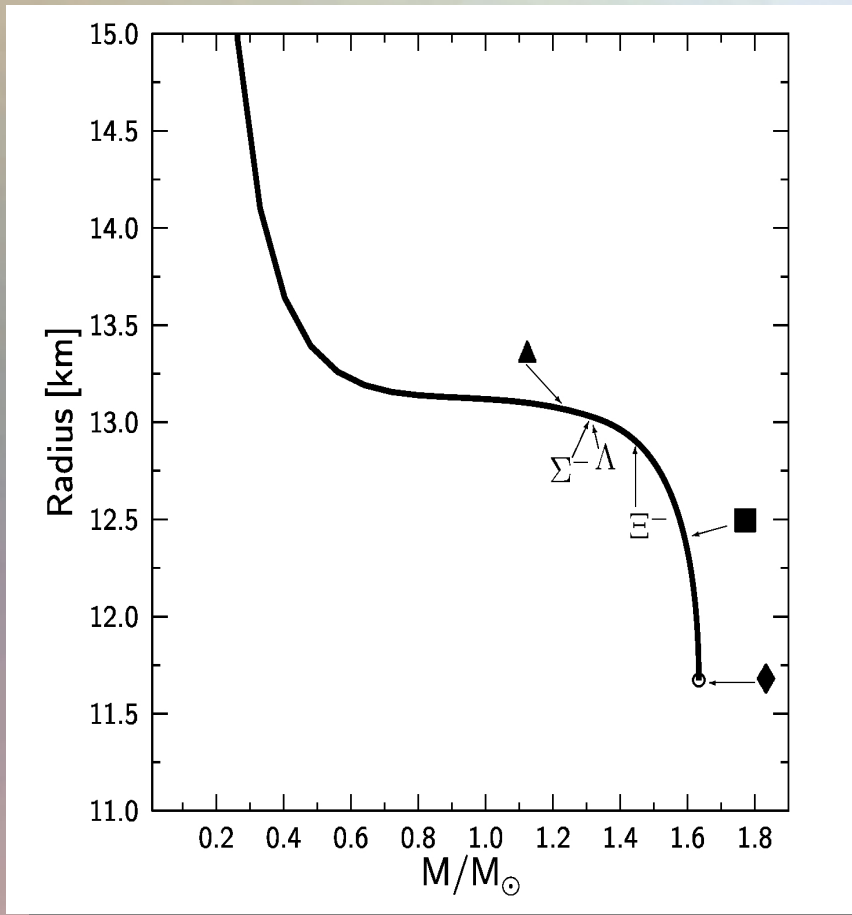

Energy density profiles of three neutron stars with different central densities and masses. The low density stars do not contain any hyperons, whereas the other two stars do have hyperons in their inner core.

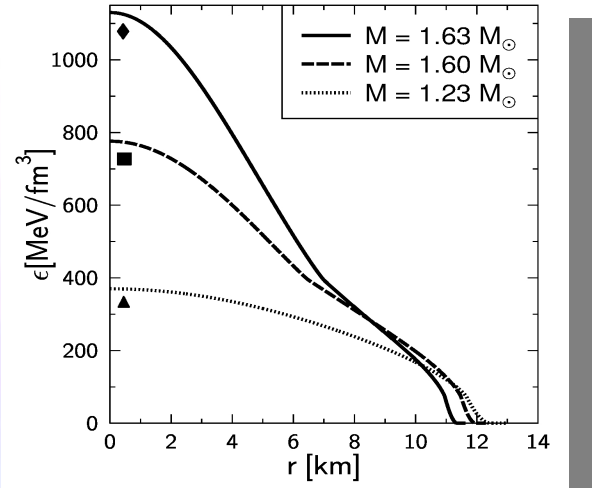

Time-time component of the metric tensor as a function of the radial coordinate. The solid line corresponds to the inner TOV-solution, whereas the doted curve depicts the outer Schwarzschild part.

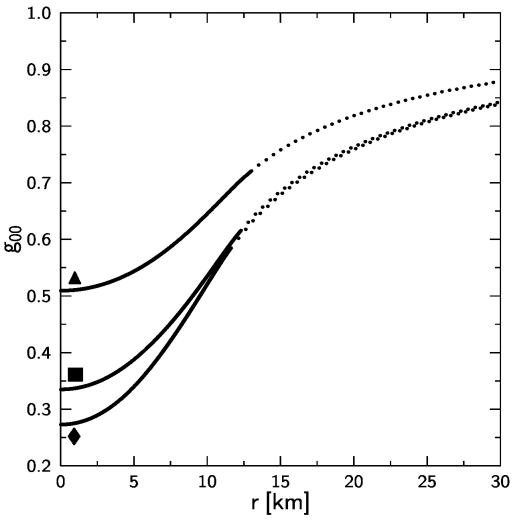

Hybrid Stars

To describe the properties of the Hadron-Quark phase transition happening in Hybrid stars an effective model for the quark phase is needed:

$$\lambda_j \equiv \lambda_{ja}{}^{b}$$

$$\begin{aligned}\mathcal{L} \;=\; & \underbrace{\overline{\psi}\,(i\,\partial\!\!\!/ - \hat{m}_0)\,\psi}_{\text{Kinetische und Massenbeiträge}} + \underbrace{G_S \sum_{j=0}^{8}\left[\left(\overline{\psi}\,\frac{\lambda_j}{2}\,\psi\right)^2 + \left(\overline{\psi}\,\frac{i\gamma_5\lambda_j}{2}\,\psi\right)^2\right]}_{\text{Skalare Wechselwirkung}} \\ & \underbrace{- G_V \sum_{j=0}^{8}\left[\left(\overline{\psi}\,\gamma_\mu\frac{\lambda_j}{2}\,\psi\right)^2 + \left(\overline{\psi}\,\gamma_\mu\frac{\gamma_5\lambda_j}{2}\,\psi\right)^2\right]}_{\text{Vektorielle Wechselwirkung}} \\ & \underbrace{- K\left[\det{}_f\left(\overline{\psi}\,(1-\gamma_5)\,\psi\right) + \det{}_f\left(\overline{\psi}\,(1+\gamma_5)\,\psi\right)\right]}_{\text{Flavour Mischterme}} + \underbrace{\mathcal{L}_L}_{\text{Leptonische Beiträge}}\end{aligned}$$

$$\psi \;\equiv\; \psi^{f}_{Aa}$$

$$\partial\!\!\!/ \equiv \partial\!\!\!/_A{}^B := \partial_\mu \gamma^\mu{}_A{}^B$$

Eg. the Nambu-Jona-Lasinio (NJL) Model or the MIT-Bag model

$$\begin{aligned}\epsilon^Q &= \sum_{f=u,d,s}\frac{\nu_f}{2\pi^2}\int_0^{k_F^f} k^2\sqrt{m_f^2+k^2}\,dk \;+ B \\ P^Q &= \sum_{f=u,d,s}\frac{\nu_f}{6\pi^2}\int_0^{k_F^f}\frac{k^4}{\sqrt{m_f^2+k^2}}\,dk \;- B\,,\end{aligned}$$

A hybrid model of a compact star is realized by a construction of a phase transition between a hadronic model and a quark model. In contrast to the Maxwell construction of a phase transition, in a Gibbs construction a mixed phase is present in the stars interior, where both phases co-exist. In the mixed phase transition region each phase has a charge; only the overall electrical charge density vanishes. In the mixed phase, the pressure of the hadronic matter has to be equal to the pressure of the quark phase, whereas the particle and energy densities differ.

M. Hanauske, L.M. Satarov, I.N. Mishustin, H. Stöcker, and W. Greiner, Phys. Rev. D 64, 043005 (2001)

The Gibbs Construction

Since the charge neutrality condition is only globally realized, the pressure depends on two independently chemical potentials, the baryonic and charge chemical potential:

$$\begin{aligned} P^H(\mu_B,\mu_e) &= P^Q(\mu_B,\mu_e)\,, \\ \mu_B = \mu_B^H &= \mu_B^Q\,, \\ \mu_e = \mu_e^H &= \mu_e^Q \end{aligned}$$

Charge density neutrality condition:

$$\rho_e := (1-\chi)\rho_e^H(\mu_B,\mu_e) + \chi\rho_e^Q(\mu_B,\mu_e) = 0\,.$$

Overall baryonic density:

$$\rho_B = (1-\chi)\rho_B^H(\mu_B,\mu_e) + \chi\rho_B^Q(\mu_B,\mu_e)\,,$$

$$\mu_i = B_i\,\mu_B + Q_i\,\mu_e$$

$$\begin{aligned} \mu_u &= \frac{1}{3}(\mu_B - 2\,\mu_e) \\ \mu_d = \mu_s &= \frac{1}{3}(\mu_B + \mu_e) \quad . \end{aligned}$$

The Gibbs Construction

Hadronic and quark surface:

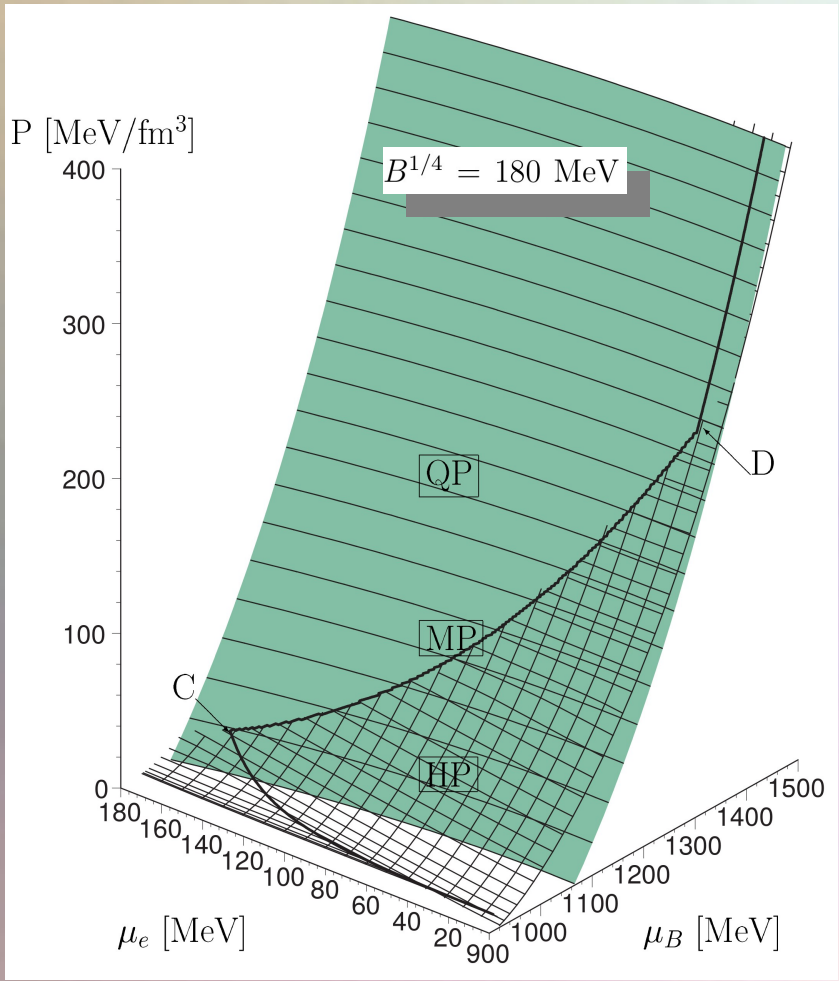

Particle composition:

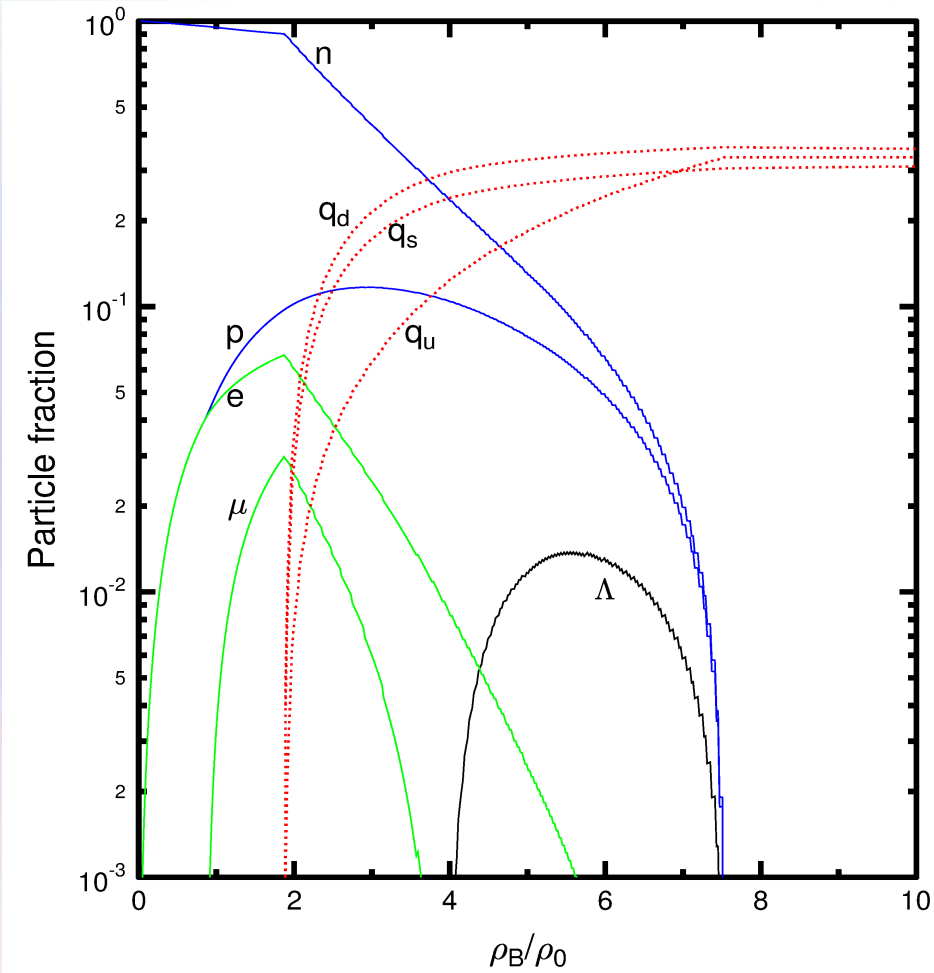

The Gibbs Construction

Hadronic and quark surface:

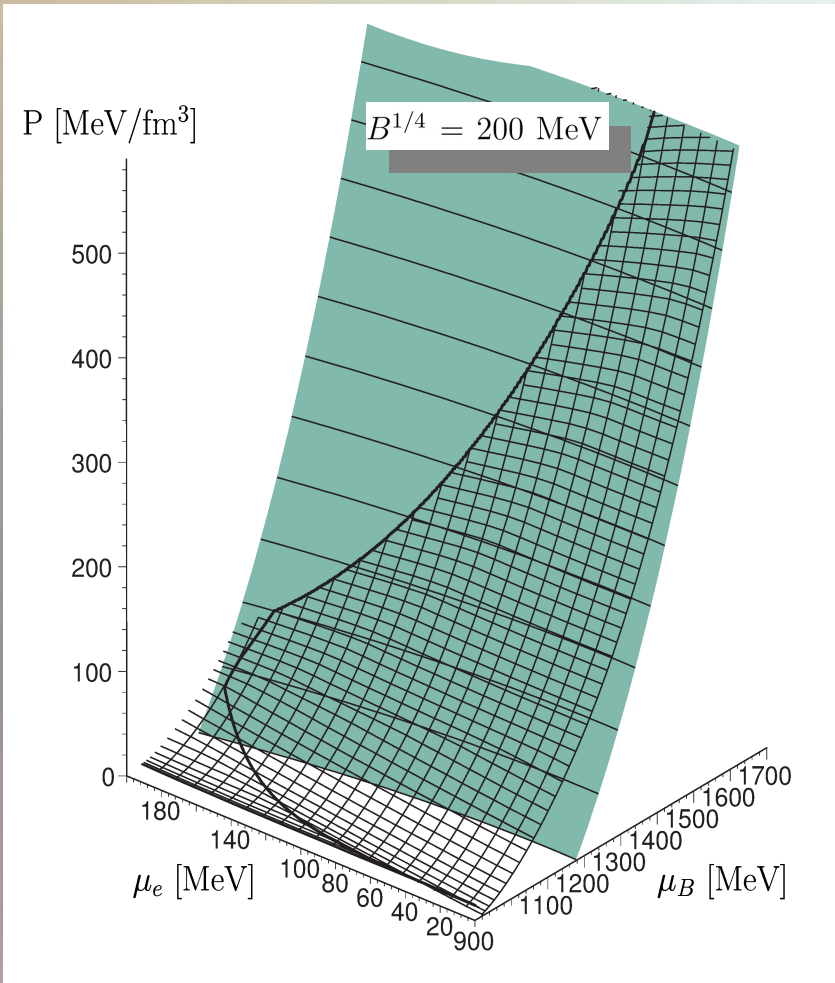

Particle composition:

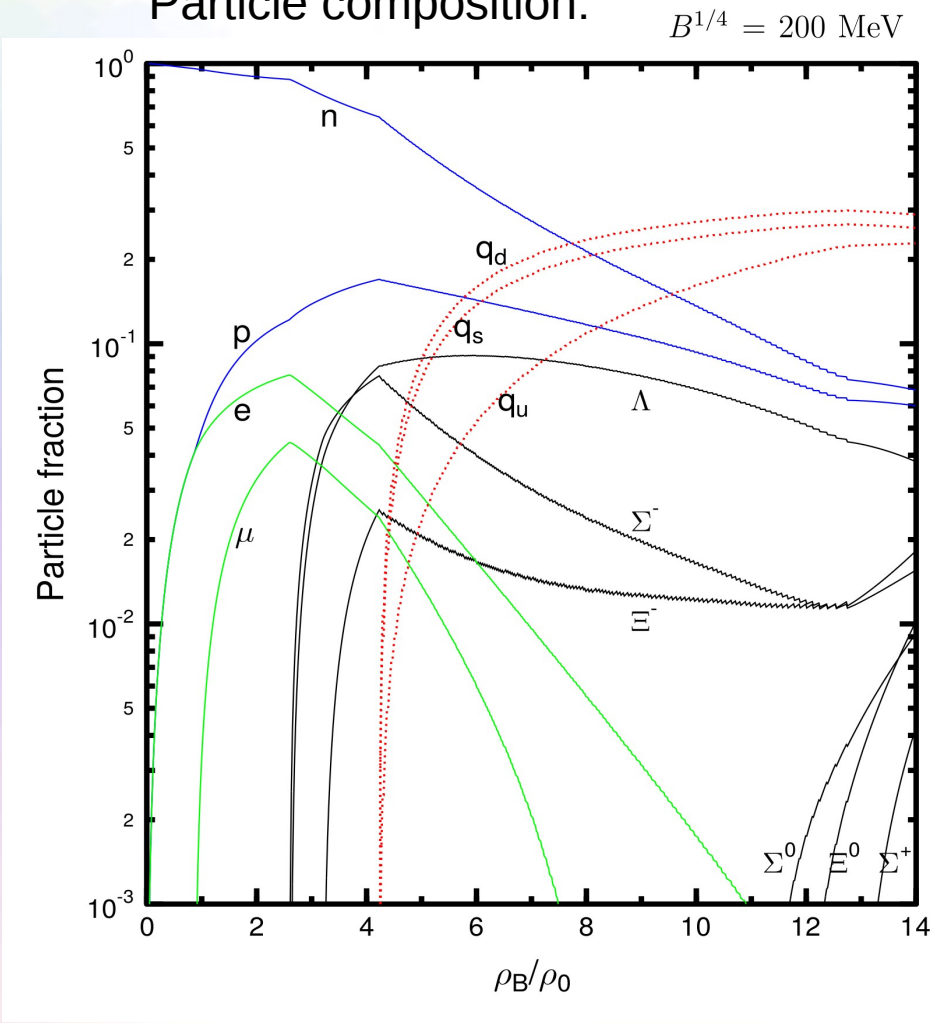

M. Hanauske, Dissertation, "Properties of Compact Stars within QCD-motivated Models"

The Gibbs Construction

$B^{1/4} = 180$ MeV

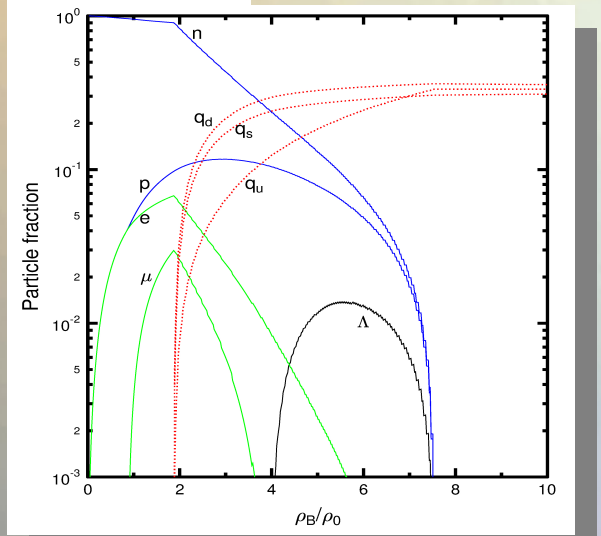

$B^{1/4} = 200$ MeV

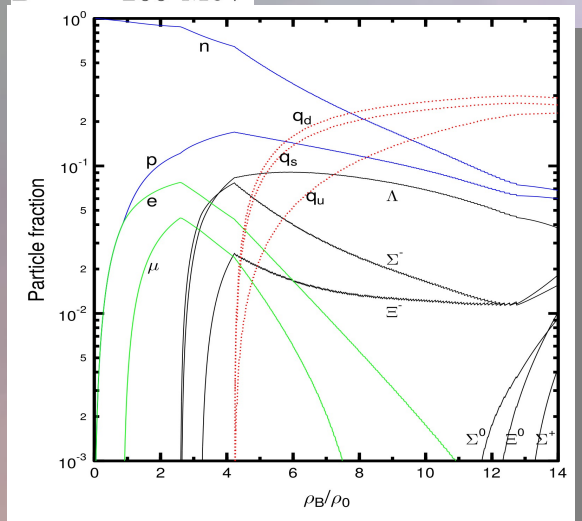

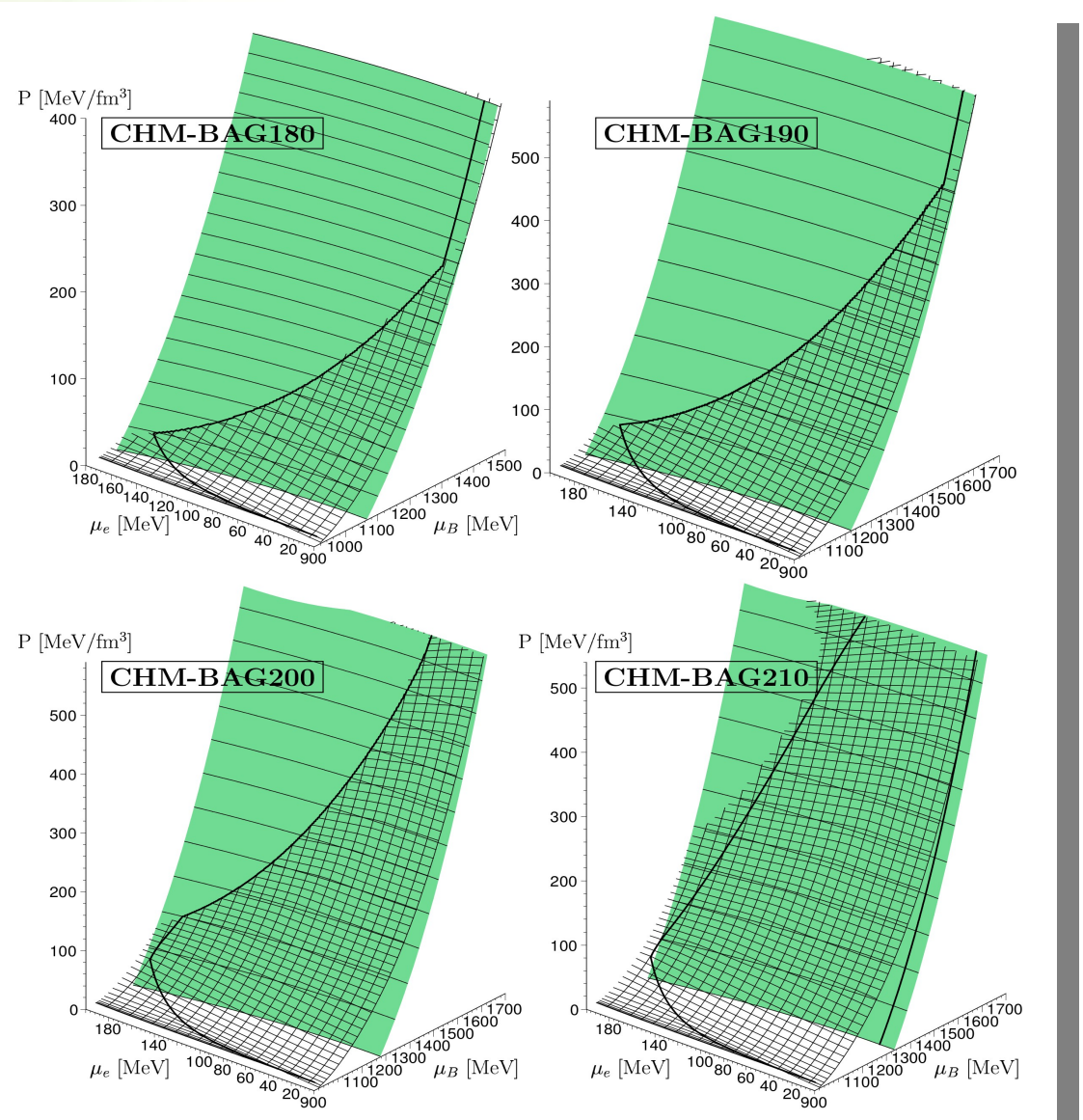

Hybrid Star Properties

Mass-Radius relations within two different hybrid star models. In both models the MIT-Bag model was used for the quark phase, whereas for the hadronic phase, the chiral hadron model (left figure) and the NLZY-model (right figure) was used.

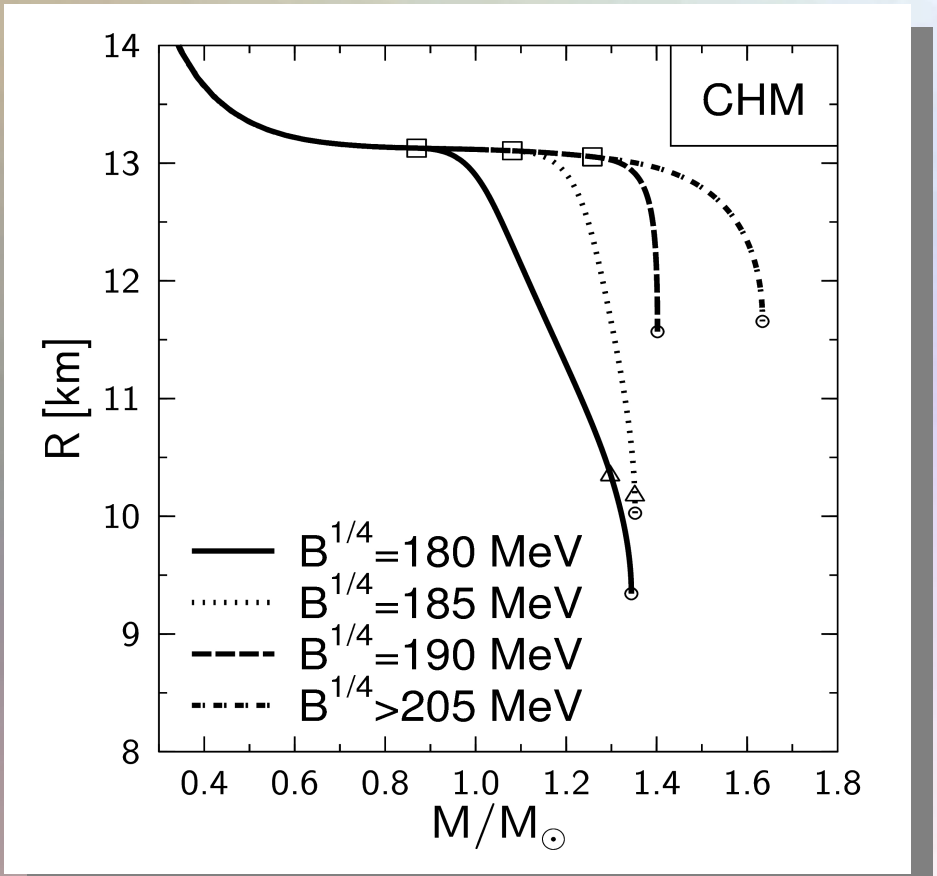

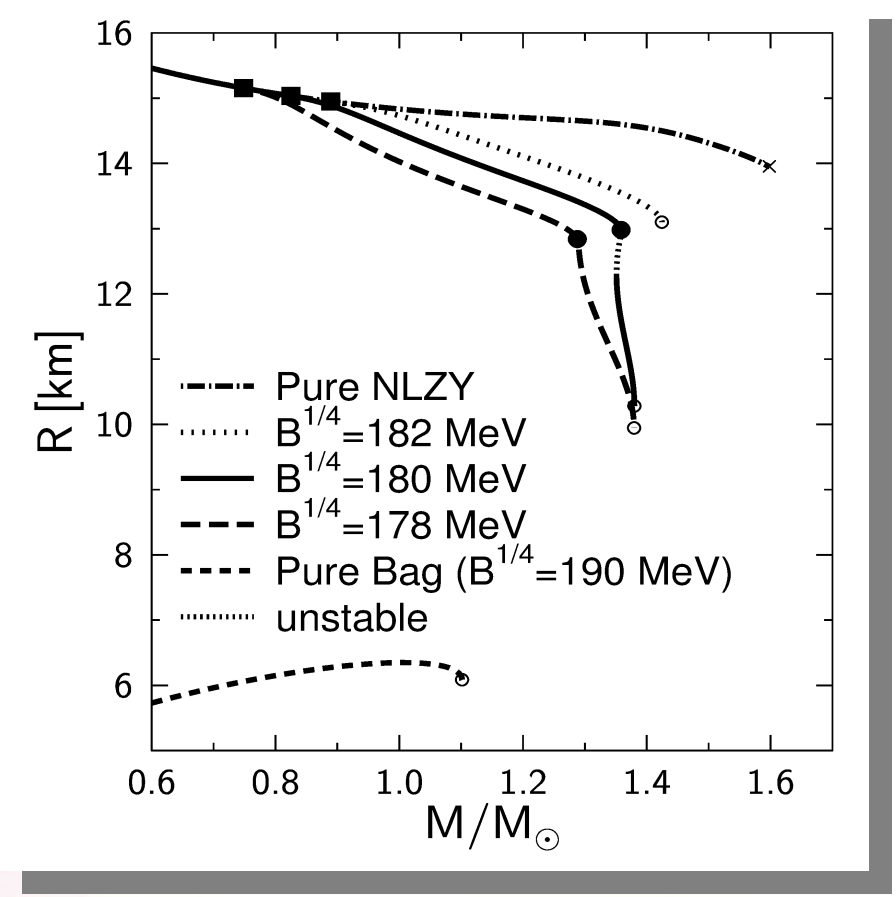

M. Hanauske, Dissertation, "Properties of Compact Stars within QCD-motivated Models"

The Twin Star Collapse

Usually it is assumed that this loss of stability leads to the collapse into a black hole. However, realistic calculations open another possibility: the collapse into the twin star on the second sequence. A star from the first sequence which reaches the maximum mass (point A) will collapse to its twin star. The latter is the corresponding star on the second sequence, i.e. the one which has the same total baryon number (point B).

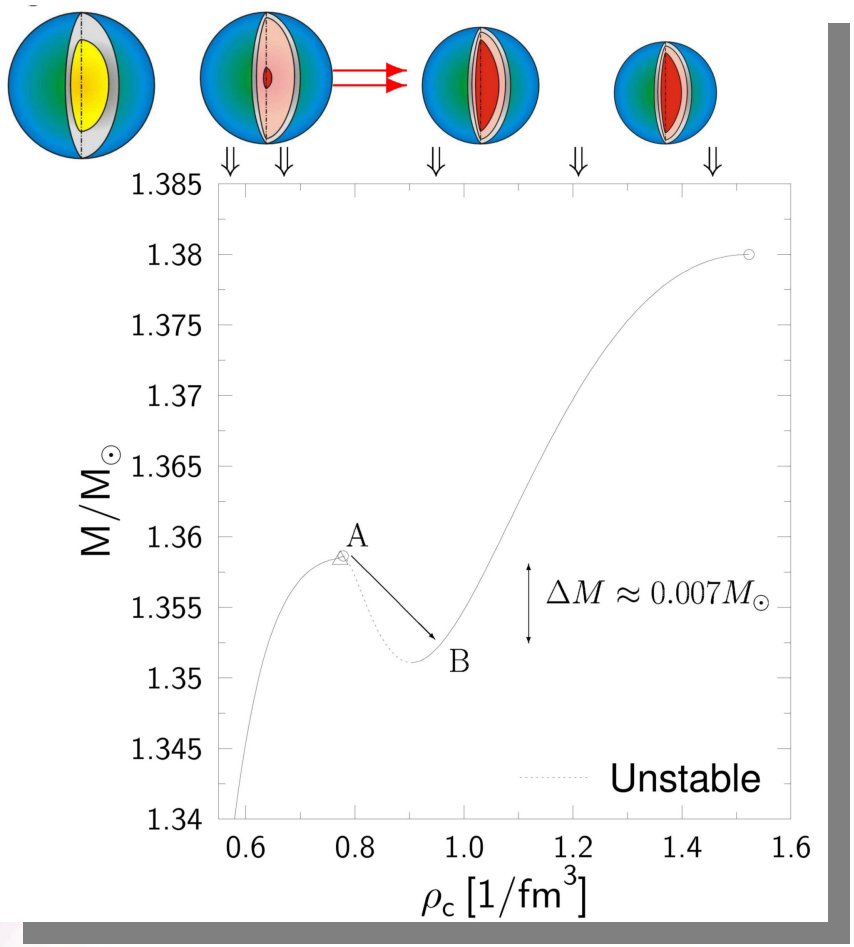

I.N. Mishustin, M. Hanauske, A. Bhattacharyya, L.M. Satarov, H. Stöcker, and W. Greiner, “Catastrophic rearrangement of a compact star due to quark core formation”, Physics Letters B 552 (2003) p.1-8

The Twin Star Collapse

Density profiles of the two twins

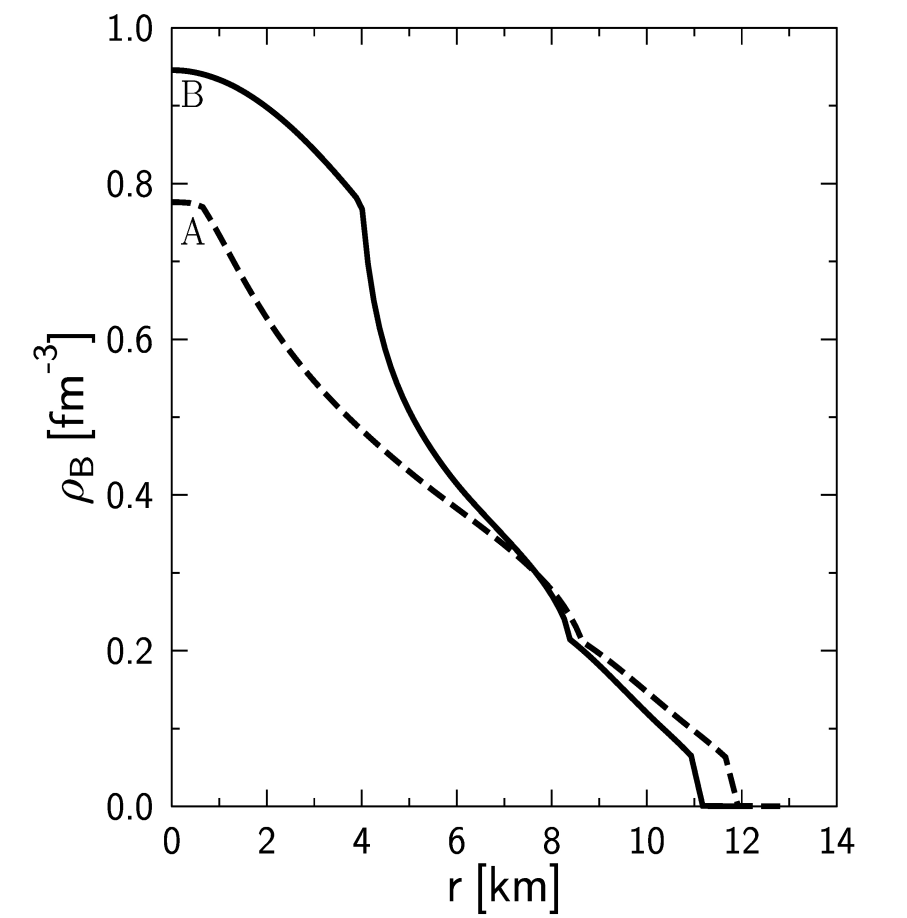

Conservation of total baryonic mass

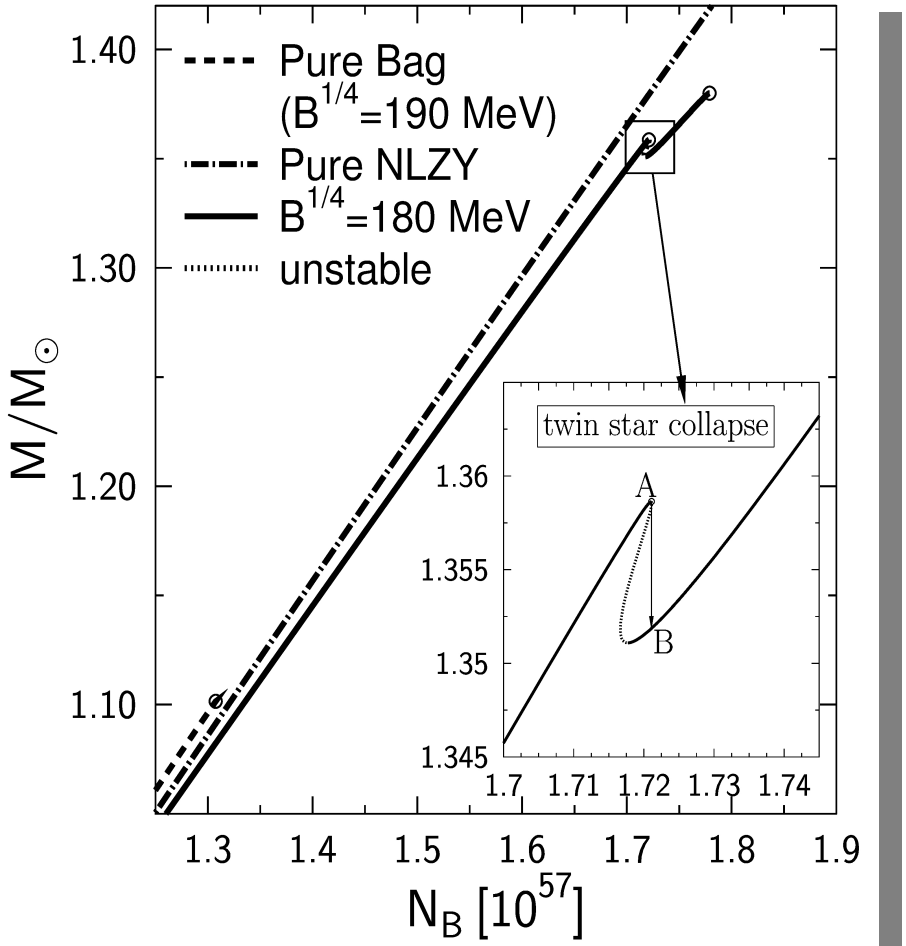

The Maxwell Construction

If the surface tension between the hadron and quark phase is relatively large, the mixed phase could completely disappear, so that a sharp boundary between the two phase appears. The Hadron-quark phase transition is then described using a Maxwell construction.

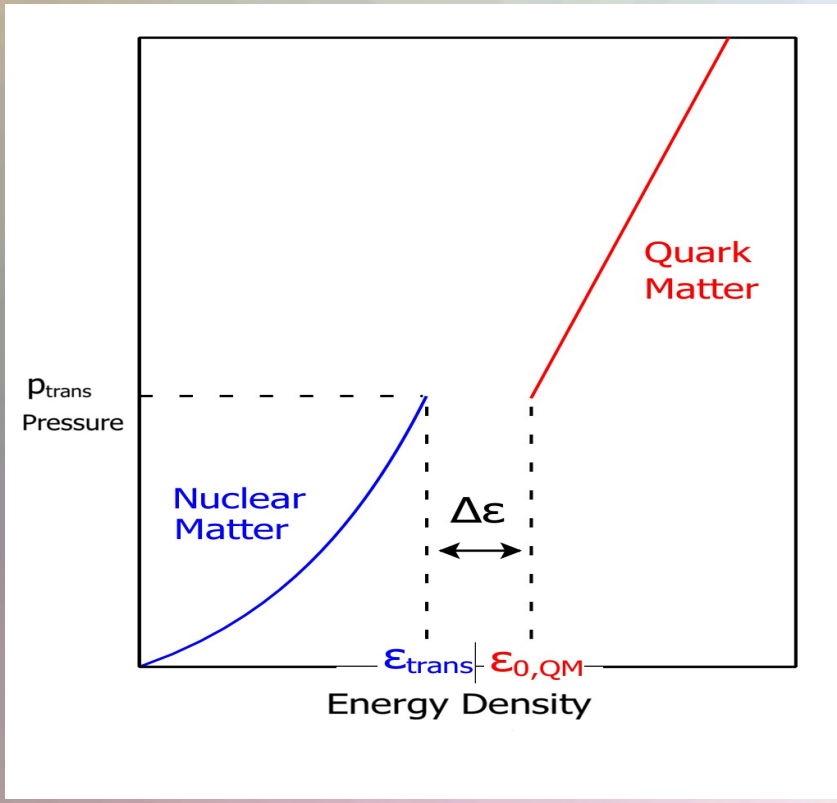

Image from M.G. Alford, S. Han, and M. Prakash, Phys. Rev. D 88, 083013 (2013)

Pressure and baryon chemical potential stays constant, while the density and the charge chemical potential jump discontinuously during the phase transition.

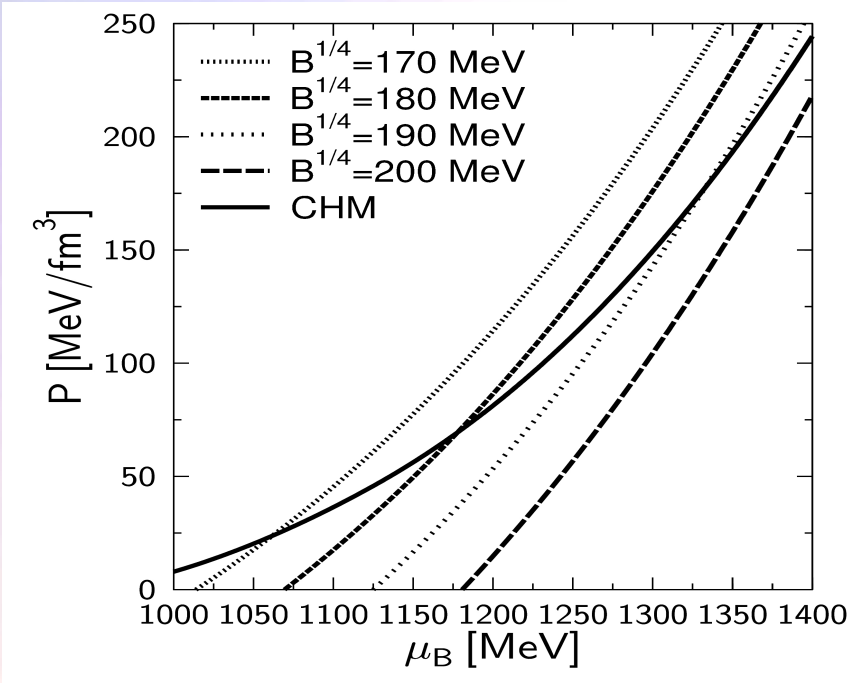

Hybrid Star Properties

In contrast to the Gibbs construction, the star's density profile within the Maxwell construction (see middle figure) will have a huge density jump at the phase transition boundary. Twin star properties can be found more easily when using a Maxwell construction (see left and right figure).

Mass-Density relation

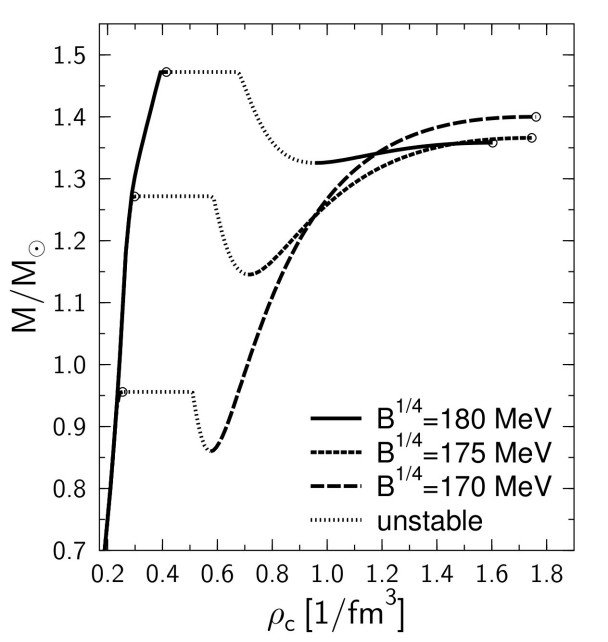

Energy-density profiles

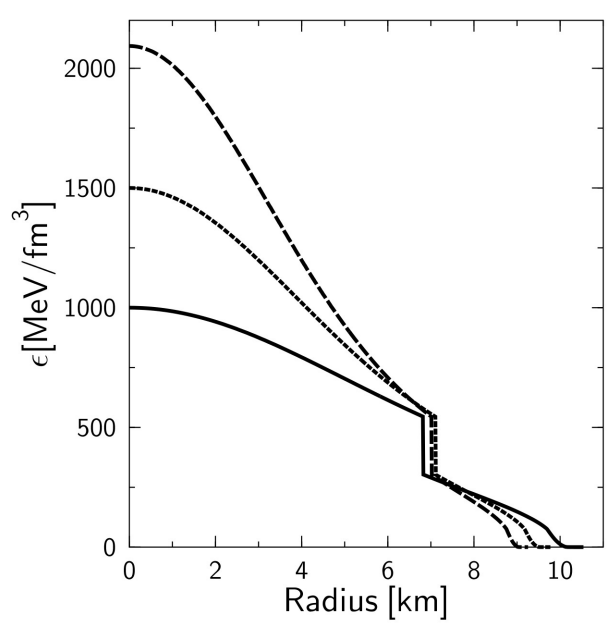

Radius-Mass relation

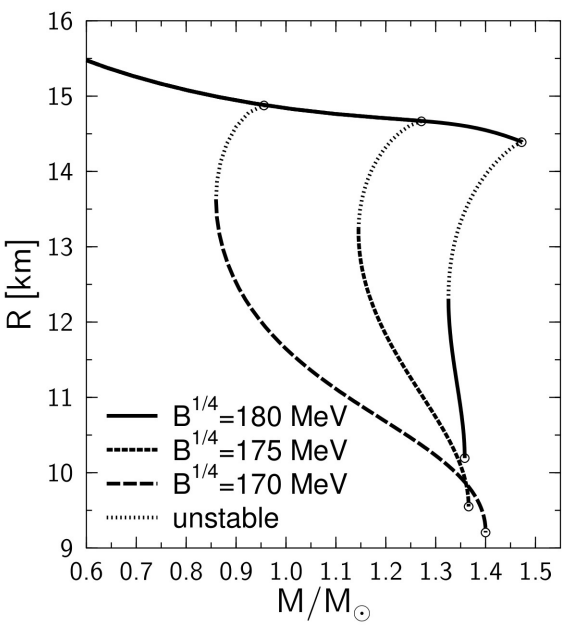

Matthias Hanauske: "How to detect the QGP with telescopes", GSI Annual Report 2003, p.96

Exotic Stars

But, unfortunately, twin stars can not be created solely by a Hadron-Quark phase transition. Extremely bound hyperon mater, or kaon condensation could also form a twin star behaviour.

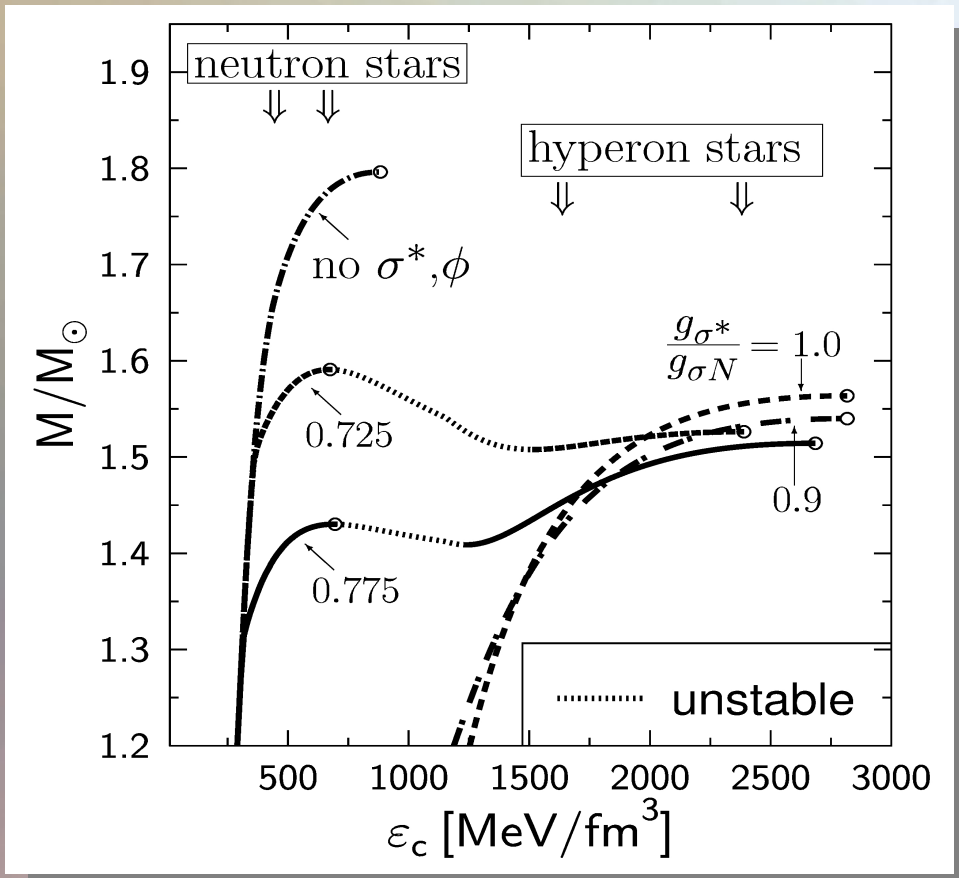

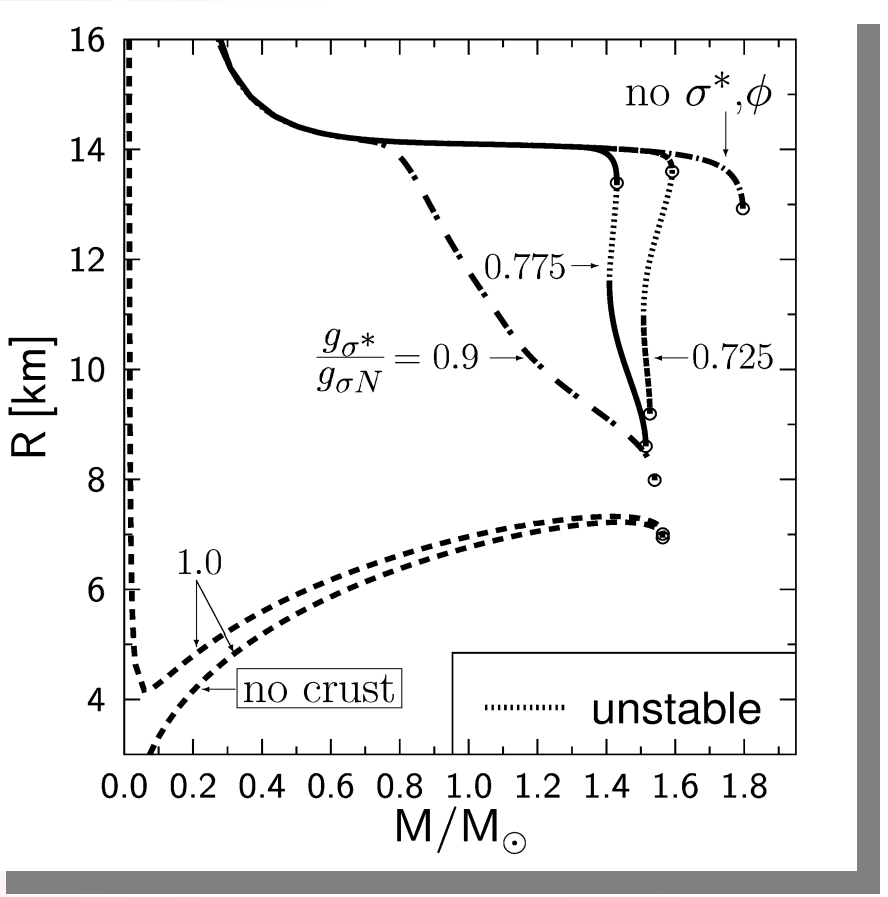

J. Schaffner-Bielich, M. Hanauske, H. Stöcker, and W. Greiner, Phys. Rev. Lett. 89, 171101 (2002)

The Spin Up Effect

A rotating neutron star slowly loses its energy and angular momentum through electromagnetic and gravitational radiation with time. However, it conserves the total baryon number during this evolution. The Figures below show results of uniformly rotating compact stars including a Bose-Einstein condensates of antikaons. The Figure on the right shows the behavior of angular velocity with angular momentum. The mass shedding limit sequence is shown by a light solid line. The stable parts of the normal and supramassive sequences are displayed by dark solid lines and the unstable parts by dotted lines. Curve II indicates a collapse of a neutron star to an exotic star belonging to the third family of compact stars.

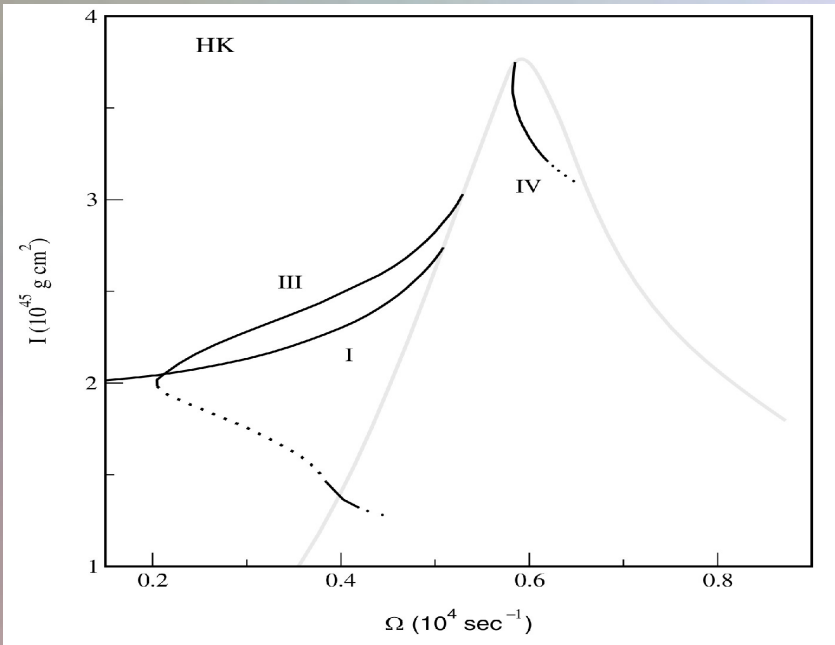

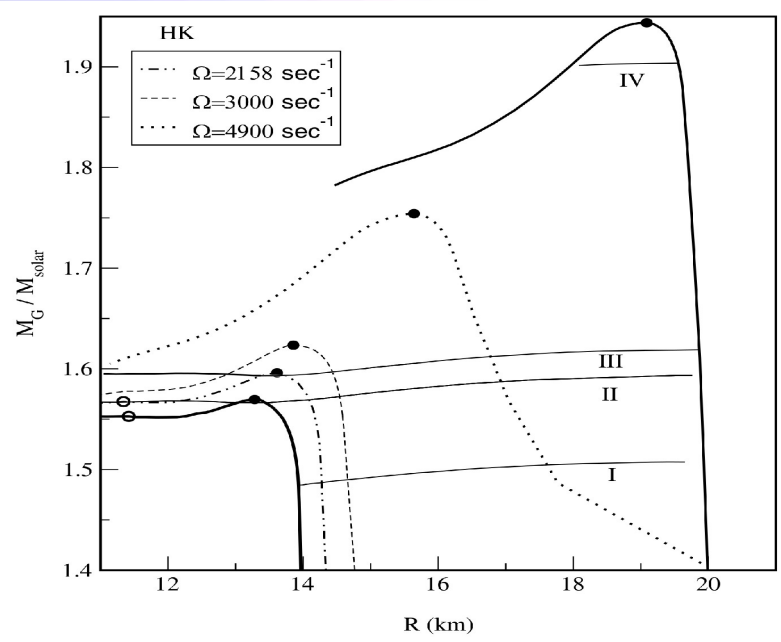

S. Banik, M. Hanauske, D. Bandyopadhyay, and W. Greiner, Phys. Rev. D 70, 123004 (2004)

Relativistic Hydrodynamics and Numerical General Relativity

A realistic numerical simulation of a twin star collapse, a merger of two compact stars or a collapse to a black hole, needs to go beyond a static, spherically symmetric TOV-solution of the Einstein- and Hydrodynamical equations.

$$R_{\mu\nu} - \frac{1}{2} g_{\mu\nu} R = 8\pi T_{\mu\nu}$$

$$\nabla_\mu (\rho u^\mu) = 0\,,$$
$$\nabla_\nu T^{\mu\nu} = 0\,.$$

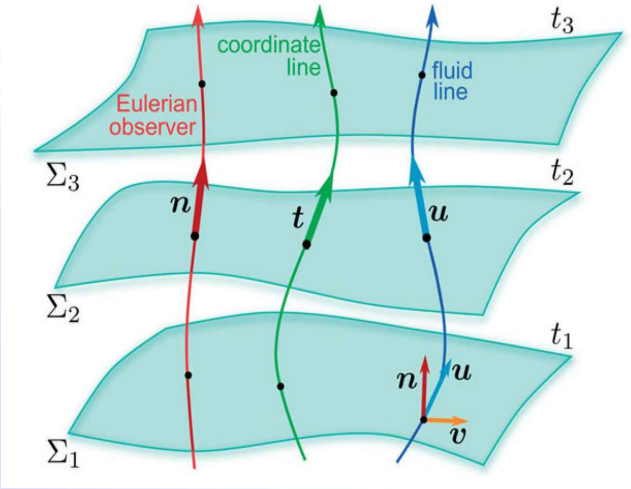

$$g_{\mu\nu} = \begin{pmatrix} -\alpha^2 + \beta_i \beta^i & \beta_i \\ \beta_i & \gamma_{ij} \end{pmatrix}$$

1. Step:

(3+1) decomposition of spacetime

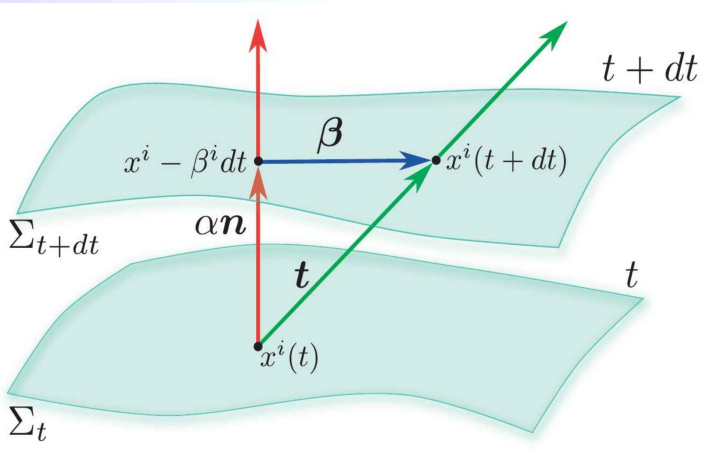

$$d\tau^2 = \alpha^2(t, x^j) dt^2$$

$$x^i_{t+dt} = x^i_t - \beta^i(t, x^j) dt$$

All figures and equations from: Luciano Rezzolla, Olindo Zanotti: Relativistic Hydrodynamics, Oxford Univ. Press, Oxford (2013)

The ADM equations

The ADM (Arnowitt, Deser, Misner) equations come from a reformulation of the Einstein equation using the (3+1) decomposition of spacetime.

$$\partial_t \gamma_{ij} = -2\alpha K_{ij} + \mathcal{L}_{\boldsymbol{\beta}} \gamma_{ij} = -2\alpha K_{ij} + D_i \beta_j + D_j \beta_i$$

$$\partial_t K_{ij} = -D_i D_j \alpha + \beta^k \partial_k K_{ij} + K_{ik} \partial_j \beta^k + K_{kj} \partial_i \beta^k + \alpha \left({}^{(3)}R_{ij} + K K_{ij} - 2 K_{ik} K^k{}_j \right) + 4\pi\alpha \left[\gamma_{ij} (S - E) - 2 S_{ij} \right]$$

Time evolving part of ADM

$$D_j (K^{ij} - \gamma^{ij} K) = 8\pi S^i$$

$${}^{(3)}R + K^2 - K_{ij} K^{ij} = 16\pi E$$

Constraints on each hypersurface

Three dimensional covariant derivative

$$D_\nu := \gamma^\mu{}_\nu \nabla_\mu = (\delta^\mu_\nu + n_\nu n^\mu) \nabla_\mu$$

Three dimensional Riemann tensor

$${}^{(3)}R^\mu{}_{\nu\kappa\sigma} = \partial_\kappa {}^{(3)}\Gamma^\mu_{\nu\sigma} - \partial_\sigma {}^{(3)}\Gamma^\mu_{\nu\kappa} + {}^{(3)}\Gamma^\mu_{\lambda\kappa} {}^{(3)}\Gamma^\lambda_{\nu\sigma} - {}^{(3)}\Gamma^\mu_{\lambda\sigma} {}^{(3)}\Gamma^\lambda_{\nu\kappa}$$

$${}^{(3)}\Gamma^\alpha_{\beta\gamma} = \frac{1}{2} \gamma^{\alpha\delta} \left(\partial_\beta \gamma_{\gamma\delta} + \partial_\gamma \gamma_{\delta\beta} - \partial_\delta \gamma_{\beta\gamma} \right)$$

Spatial and normal projections of the energy-momentum tensor:

$$S_{\mu\nu} := \gamma^\alpha{}_\mu \gamma^\beta{}_\nu T_{\alpha\beta}\,,$$
$$S_\mu := -\gamma^\alpha{}_\mu n^\beta T_{\alpha\beta}\,,$$
$$S := S^\mu{}_\mu\,,$$
$$E := n^\alpha n^\beta T_{\alpha\beta}\,,$$

Extrinsic Curvature:

$$K_{\mu\nu} := -\gamma^\lambda{}_\mu \nabla_\lambda n_\nu$$

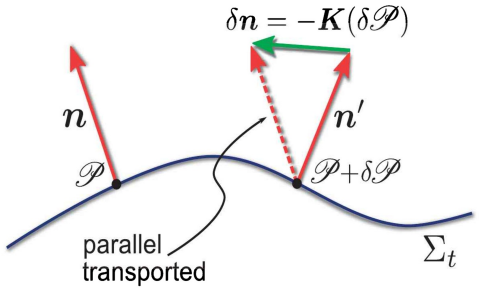

All figures and equations from: Luciano Rezzolla, Olindo Zanotti: Relativistic Hydrodynamics, Oxford Univ. Press, Oxford (2013)

From ADM to BSSNOK

Unfortunately the ADM equations are only weakly hyperbolic (mixed derivatives in the three dimensional Ricci tensor) and therefore not "well posed". It can be shown that by using a conformal traceless transformation, the ADM equations can be written in a hyperbolic form. This reformulation of the ADM equations is known as the BSSNOK (Baumgarte, Shapiro, Shibata, Nakamuro, Oohara, Kojima) formulation of the Einstein equation. Most of the numerical codes use this (or the CCZ4) formulation.

The 3+1 Valencia Formulation of the Relativistic Hydrodynamic Equations

$$\nabla_\mu(\rho u^\mu) = 0\,,$$
$$\nabla_\nu T^{\mu\nu} = 0\,.$$

To guarantee that the numerical solution of the hydrodynamical equations (the conservation of rest mass and energy-momentum) converge to the right solution, they need to be reformulated into a conservative formulation. Most of the numerical “hydro codes” use here the 3+1 Valencia formulation.

Finite difference methods

Discretisation of a hyperbolic initial value boundary problem.

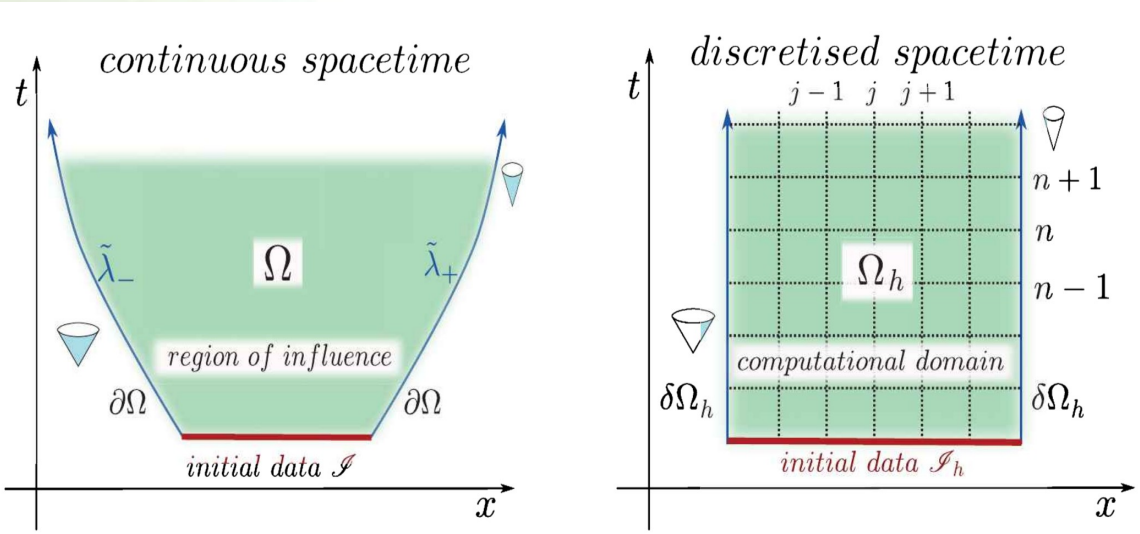

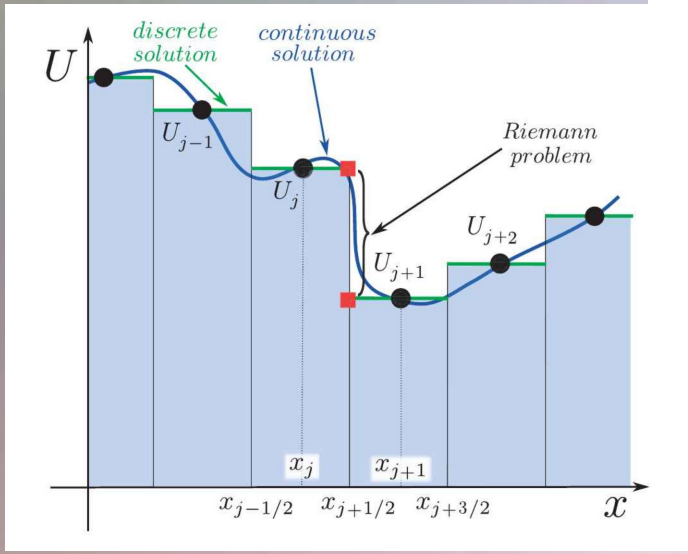

High resolution shock capturing methods (HRSC methods) are needed, when Riemann problems of discontinuous properties and shocks needs to be evolved accurately

All figures from: Luciano Rezzolla, Olindo Zanotti: Relativistic Hydrodynamics, Oxford Univ. Press, Oxford (2013)

Mergers of two Hybrid Stars

One of the planned project deals with the numerical simulation of a hybrid star merger. During the merger process the mixed and probable also the pure quark phase is present in the inner core of the hypermassive compact star. The frequency spectrum of the emitted gravitational wave reflects some of the properties of the equation of state (see presentation by Filippo Galeazzi and Kentaro Takami on Friday). Whether a Hadron-Quark phase transition is present during merger should be visible using gravitational wave detectors.

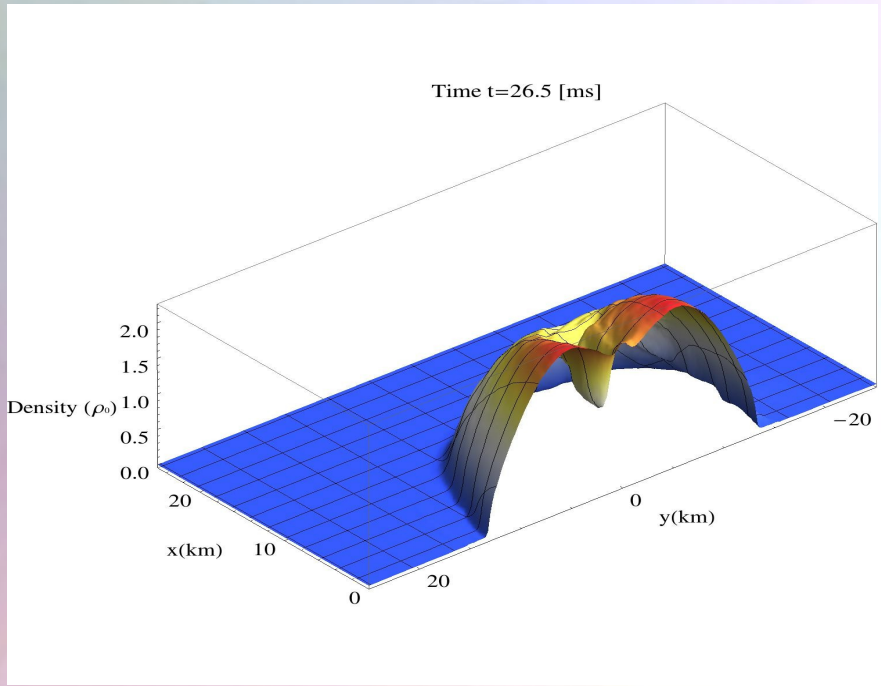

Simulations done by Kentaro Takami

Mergers of two Neutron Stars

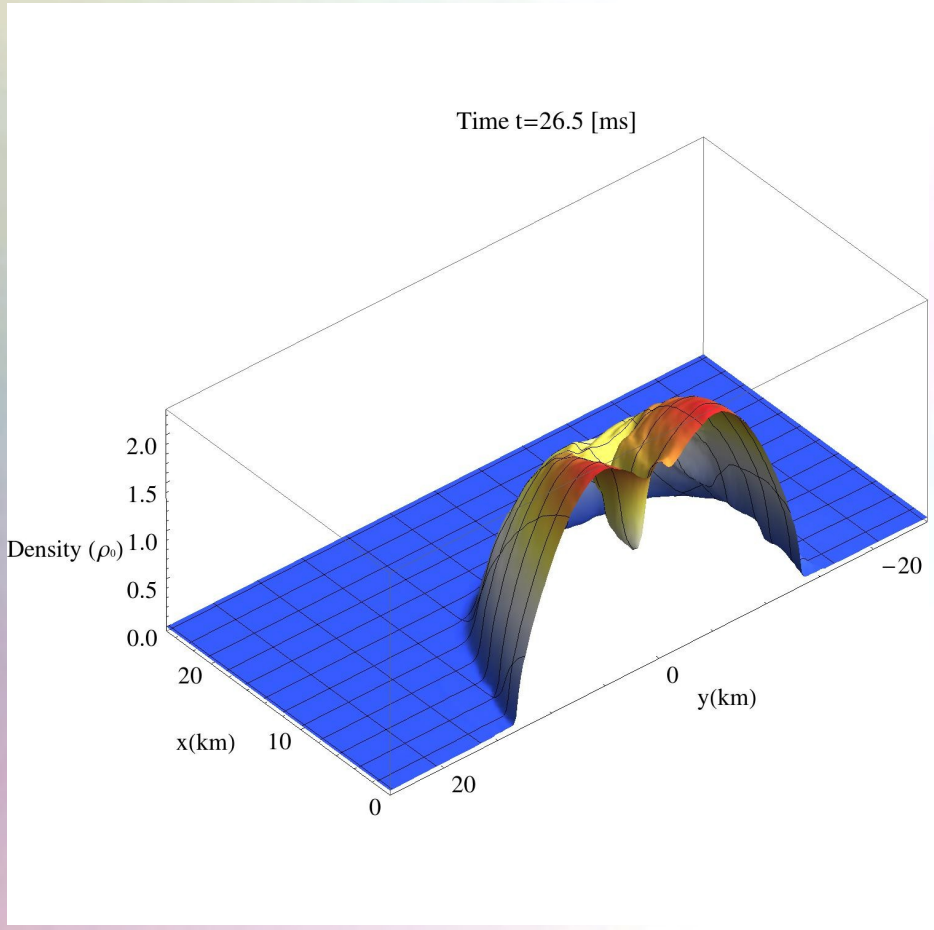

Simulations done by Kentaro Takami

Mergers of two Neutron Stars

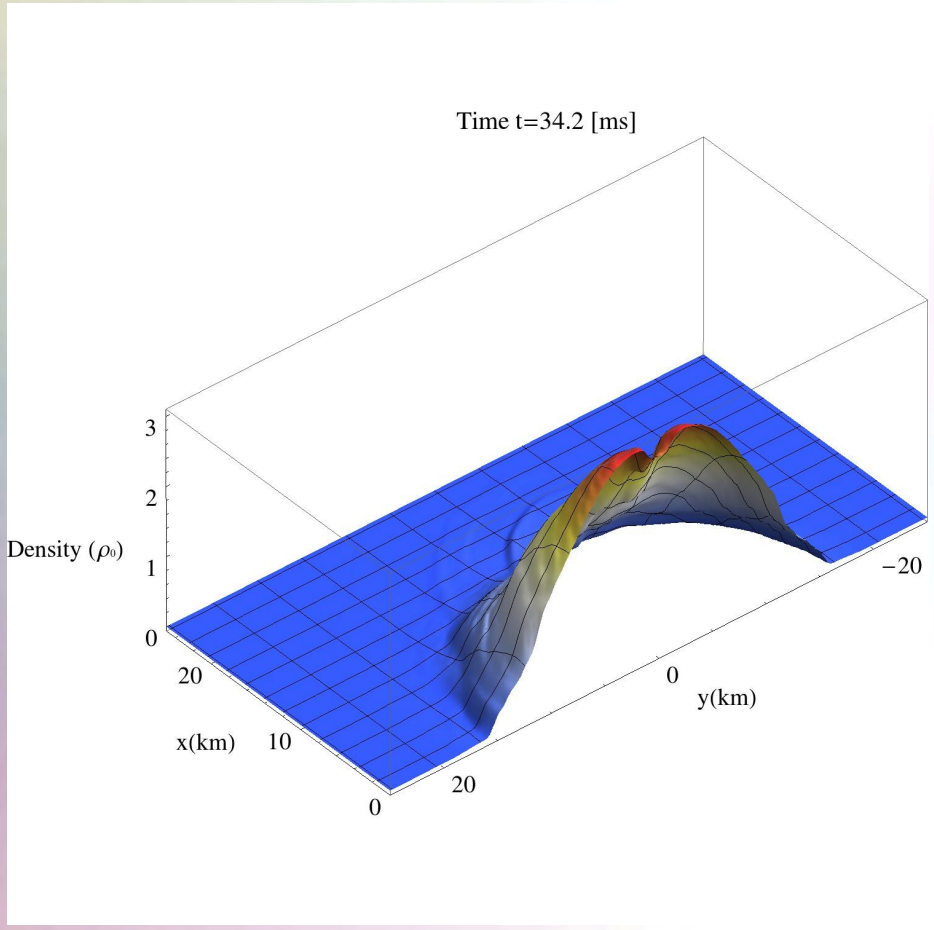

Simulations done by Kentaro Takami

Mergers of two Neutron Stars

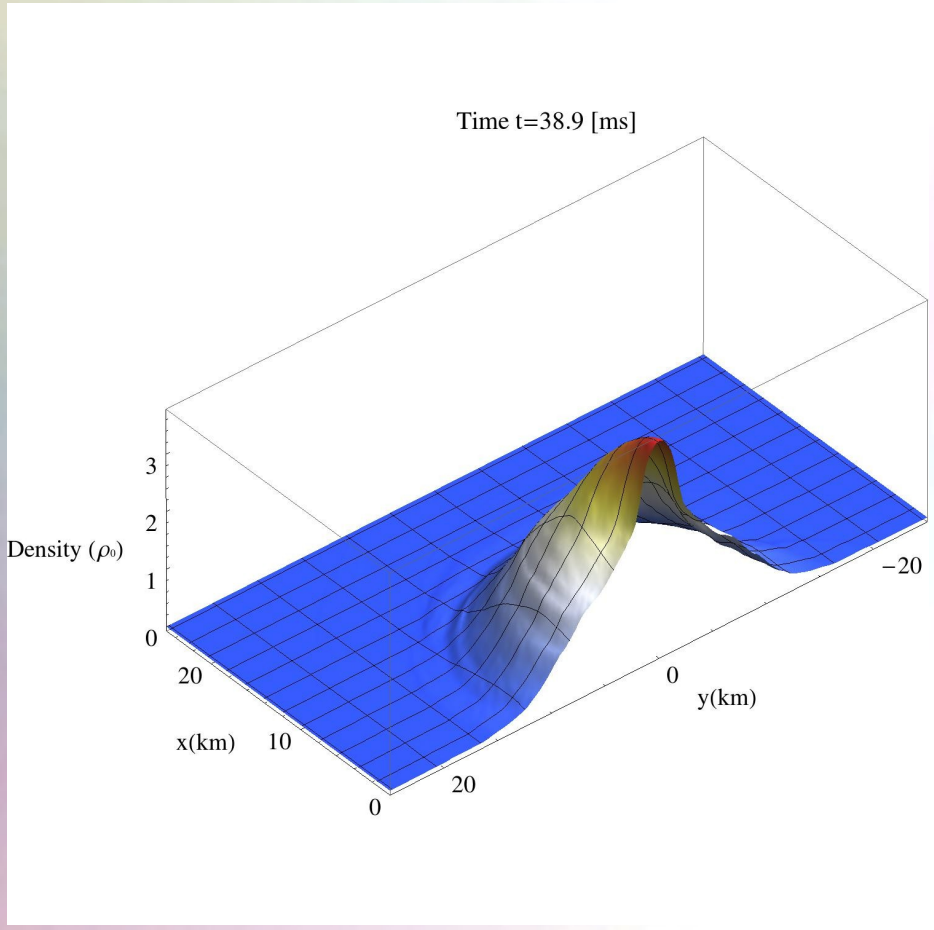

Simulations done by Kentaro Takami

Mergers of two Neutron Stars

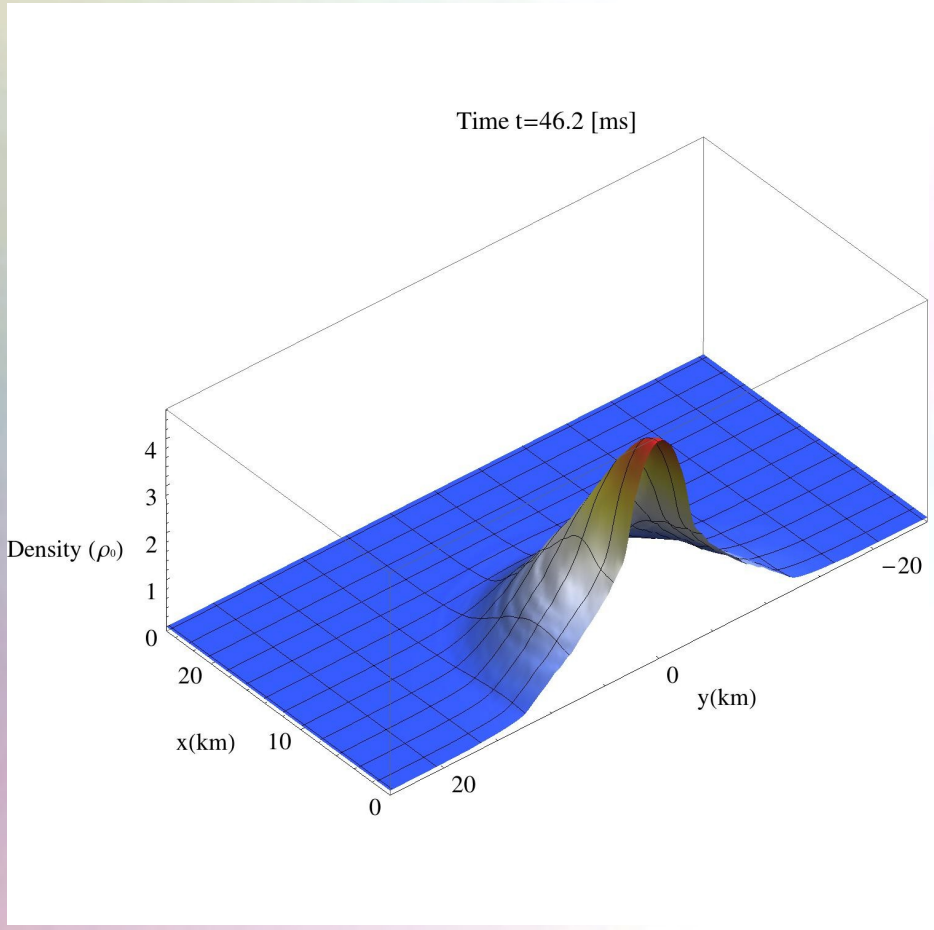

Simulations done by Kentaro Takami

Mergers of two Neutron Stars

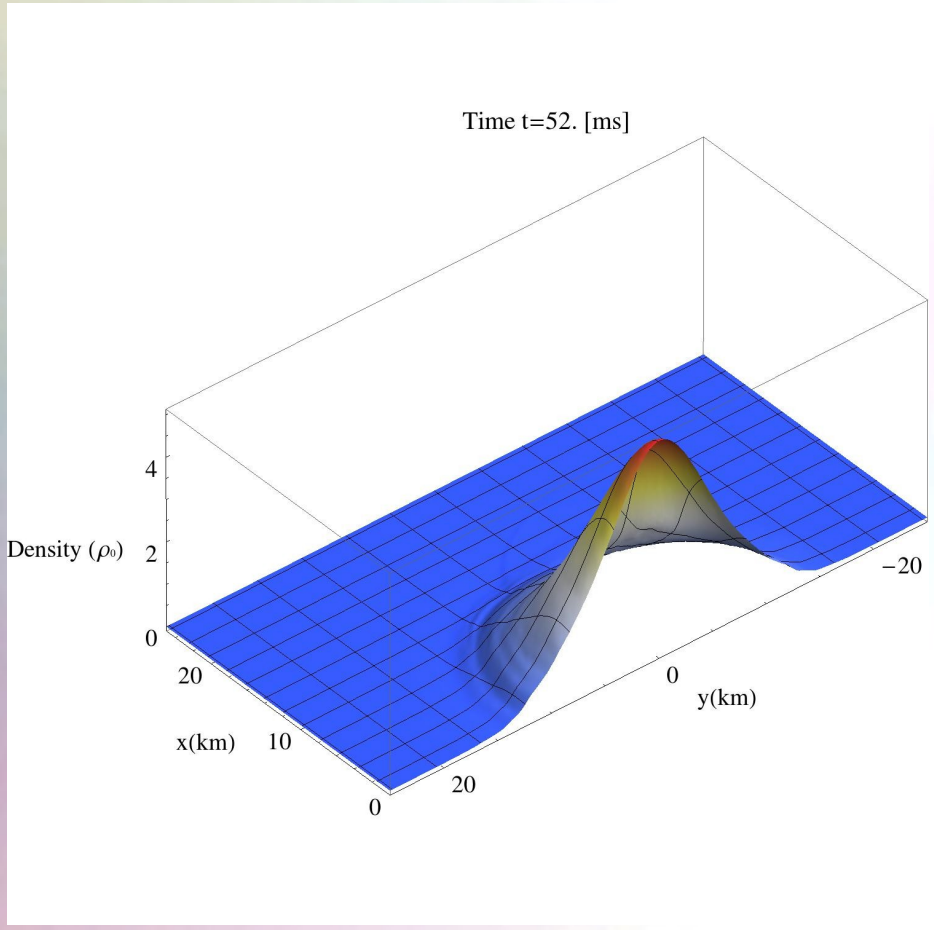

Simulations done by Kentaro Takami

Mergers of two Neutron Stars

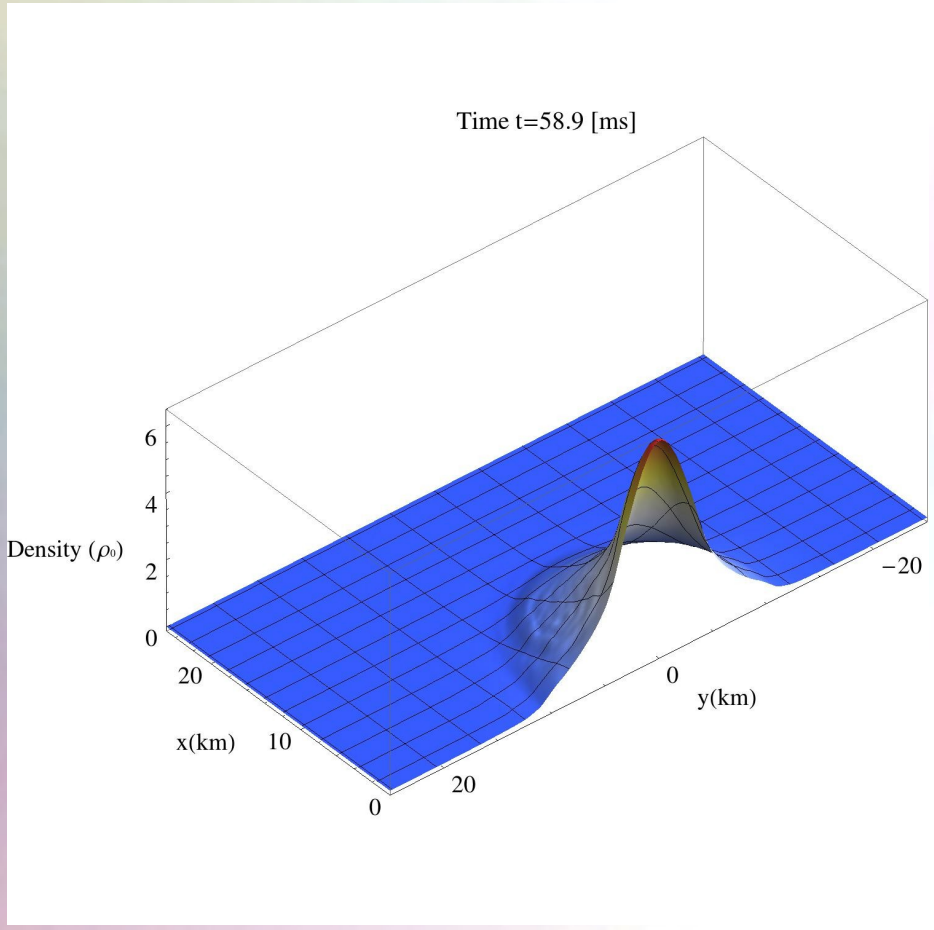

Simulations done by Kentaro Takami

Mergers of two Neutron Stars

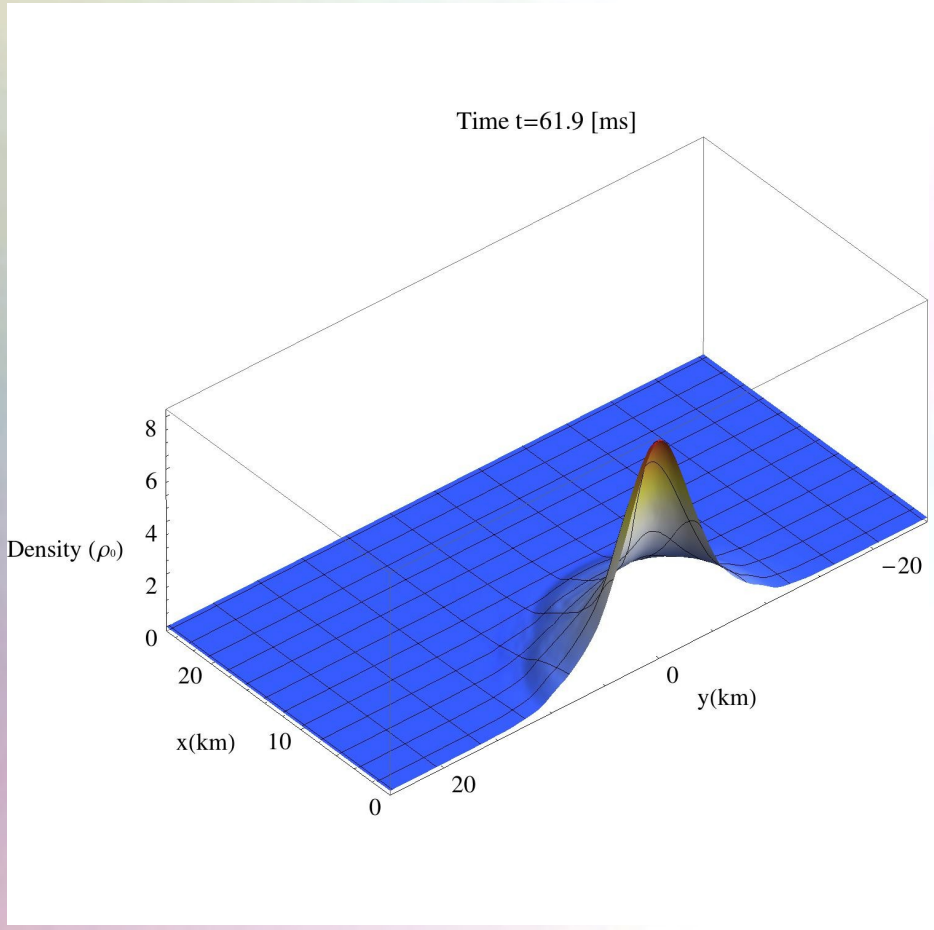

Mergers of two Neutron Stars

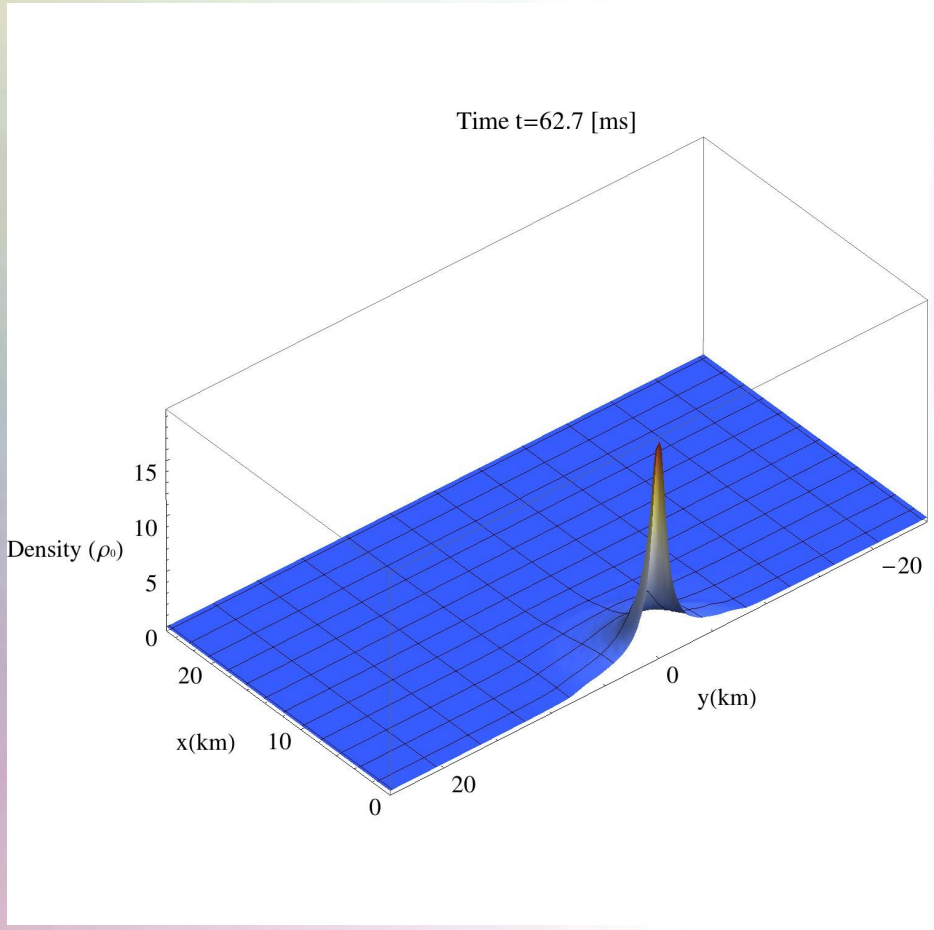

Mergers of two Neutron Stars

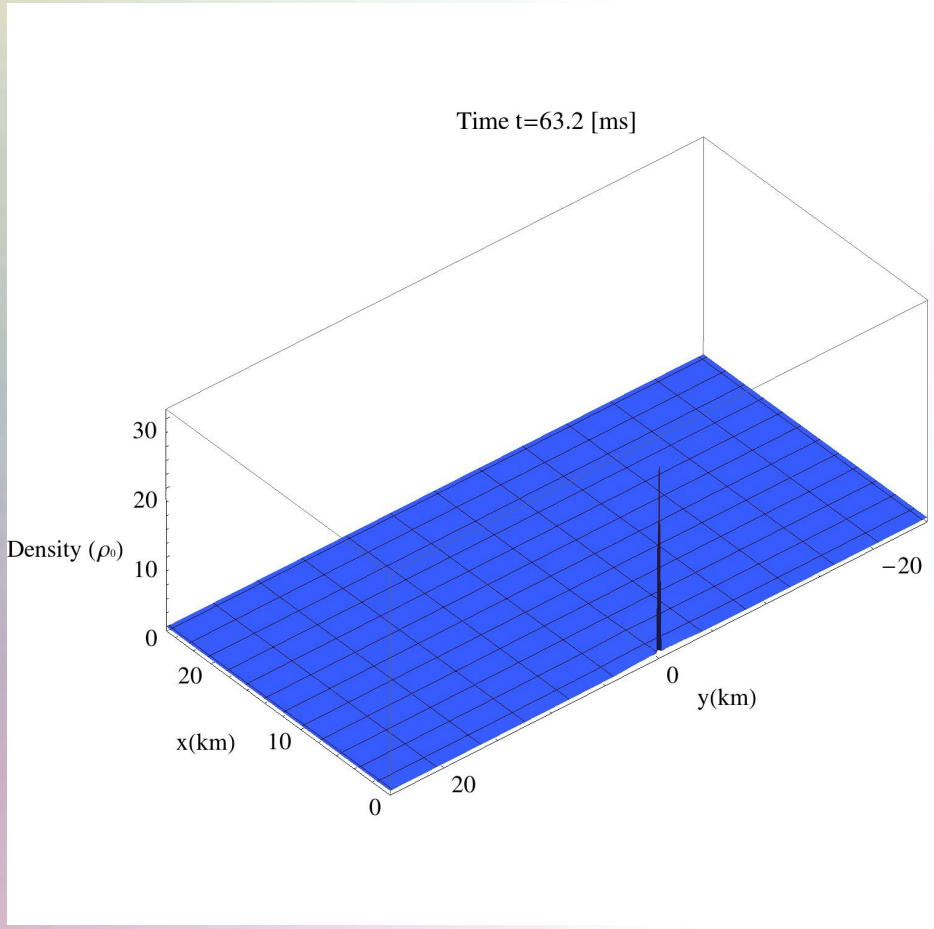

Simulations done by Kentaro Takami

Collapse Scenario of a Hybrid Star

The gravitational collapse of a hybrid star to a black hole is visualized on the right side within a space-time diagram of the Schwarzschild metric in advanced Eddington-Finkelstein coordinates.

Such a dynamical collapse could happen if a hybrid star reaches its maximum mass limit or during the final stages of a neutron star – neutron star collision after the formation of the hypermassive compact star.

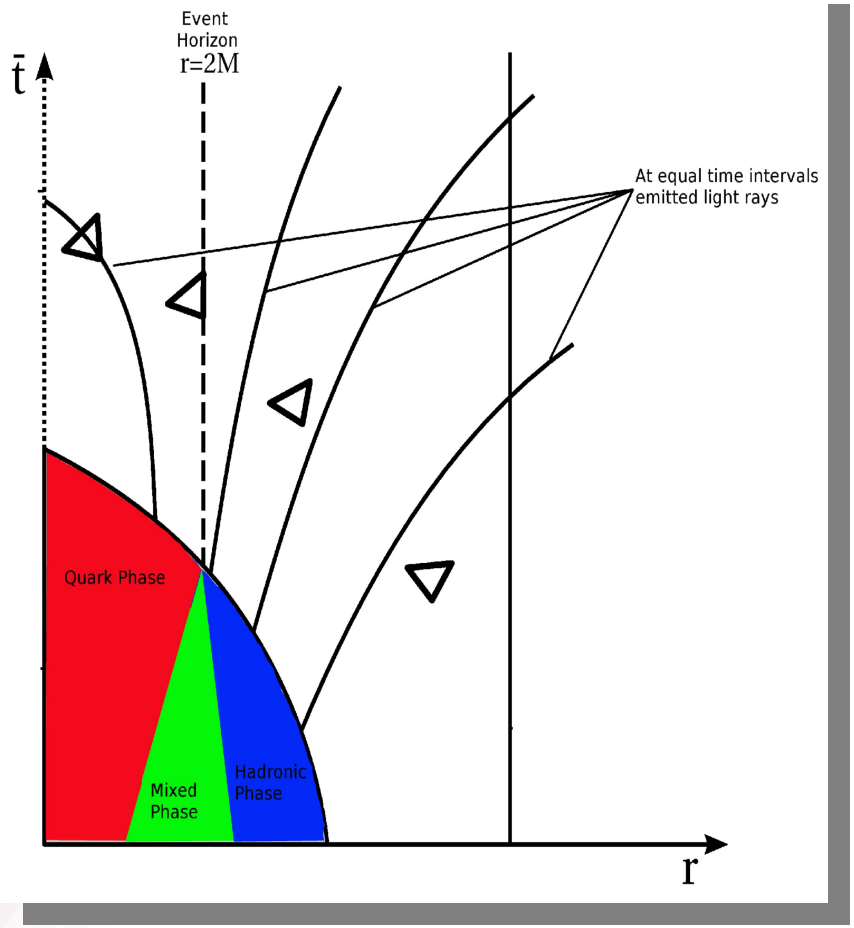

M. Hanauske, Dissertation: "Properties of Compact Stars within QCD-motivated Models" ;
University Library Publication 2004 (urn:nbn:de:hebis:30-0000005872)